People`s Democratic Republic of Algeria

Ministry of Higher Education and Scientific Research

University of Echahid Hamma Lakhdar - El Oued

Faculty of Technology

Department of Mechanical Engineering Dissertation

ACADEMIC MASTER

Domain: **Science and Technology** Division: **Mechanical Engineering**

Specialty: Electromechanical

Presented by:

BADJADI Mohammed Lamine

Entitled:

Advanced Control Strategies for PMSM Generators Using Optimization Methods

Dissertation Submitted in Partial Fulfillment of the Requirements for the Master

MEM

Degree in …………

6Publicly defended in: ……/…… /202

Board of Examiners:

Dr. ………………………………..……. Chairman

Dr. ………………………………..……. Supervisor

Dr. ………………………………..……. Examiner

University Season: 2025-2026

Thanks

First and foremost, praise be to Allah, who granted me the strength, patience, and perseverance necessary to accomplish this work.

I would like to express my special gratitude to my parents for their continuous support, care, and encouragement throughout my academic journey.

I would also like to extend my sincere thanks and appreciation to my supervisor, **Dr. BenAmor Afaf**, for her valuable guidance, insightful advice, and constant support, which greatly contributed to the completion of this dissertation.

I would like to express my deep gratitude to all the professors who contributed to my education throughout my years of study at the University of Echahid Hamma Lakhdar – El Oued, for the quality of education and valuable knowledge they provided.

My sincere thanks also go to the members of the examination committee for honoring me by accepting to evaluate and discuss this work.

Finally, I would like to express my heartfelt gratitude to everyone who contributed, directly or indirectly, to the completion of this dissertation.

DEDICATION

To the source of my strength and the reason for my perseverance, my beloved Parents, whose prayers and sacrifices paved the way for my success.

To my Sisters and Brothers, for their constant encouragement and for being the light during my darkest hours of study.

To all my Teachers and Mentors, who shared their knowledge and wisdom to shape my intellectual path.

To my Friends and Colleagues, with whom I shared the challenges and triumphs of this academic journey.

Finally, to everyone who believed in me when I doubted myself, and to my homeland, I dedicate this work as a symbol of gratitude and a step toward a brighter future.

Abstract

Abstract

This work aims to study and model a wind energy conversion system based on a Permanent Magnet Synchronous Generator (PMSG), owing to its high efficiency and suitability for renewable energy applications. The fundamental principles of wind energy systems are presented, and a mathematical model of both the generator and the wind turbine is developed in the dq reference frame.

A Field-Oriented Control (FOC) strategy based on PI controllers is also investigated to ensure effective generator control and improve its dynamic performance. In addition, intelligent optimization techniques, namely Grey Wolf Optimization (GWO) and Fuzzy Logic, are introduced to enhance the control system performance. The proposed models and control strategies are implemented and simulated using MATLAB/Simulink.

Keywords:

Wind Energy, Permanent Magnet Synchronous Generator (PMSG), Field-Oriented Control (FOC), PI Controller, Grey Wolf Optimization (GWO), Fuzzy Logic, MATLAB/Simulink, Wind Energy Conversion Systems.

الملخص

يهدف هذا العمل إلى دراسة ونمذجة نظام تحويل طاقة الرياح المعتمد على المولد المتزامن ذو المغناطيس الدائم (PMSG)، لما يتميز به من كفاءة عالية وملاءمة لتطبيقات الطاقات المتجددة. تم عرض المبادئ الأساسية لأنظمة طاقة الرياح، بالإضافة إلى تطوير نموذج رياضي للمولد والتوربين الهوائي في المرجع الدوار (dq).

كما تمت دراسة استراتيجية التحكم الموجه بالمجال (FOC) باستخدام متحكمات PI لضمان التحكم الفعال في المولد وتحسين أدائه الديناميكي. بالإضافة إلى ذلك، تم تقديم تقنيات التحسين الذكية، والمتمثلة في خوارزمية الذئب الرمادي (GWO) والمنطق الضبابي (Fuzzy Logic)، بهدف تطوير أداء نظام التحكم. وقد تم تنفيذ النماذج والاستراتيجيات المقترحة باستخدام برنامج MATLAB/Simulink.

الكلمات المفتاحية:

طاقة الرياح, المولد المتزامن دو المغناطيس الدائم (PMSG), التحكم الموجه بالمجال (FOC), المتحكم PI, خوارزمية الذئاب الرمادية (GWO), المنطق الضبابي, أنظمة طاقة الرياح

Résumé

Ce travail vise à étudier et à modéliser un système de conversion d'énergie éolienne basé sur un Générateur Synchrone à Aimants Permanents (PMSG), en raison de son rendement élevé et de son adaptation aux applications des énergies renouvelables. Les principes fondamentaux des systèmes éoliens sont présentés, puis un modèle mathématique du générateur et de la turbine éolienne est développé dans le repère dq.

Une stratégie de commande orientée champ (FOC) utilisant des régulateurs PI est également étudiée afin d'assurer un contrôle efficace du générateur et d'améliorer ses performances dynamiques. En outre, des techniques d'optimisation intelligentes, notamment l'algorithme Grey Wolf Optimization (GWO) et la logique floue (Fuzzy Logic), sont introduites dans le but d'améliorer les performances du système de commande. Les modèles et stratégies proposés sont implémentés et simulés sous MATLAB/Simulink.

Mots-clés:

Énergie éolienne, Générateur Synchrone à Aimants Permanents (PMSG), Commande Orientée Champ (FOC), Régulateur PI, Grey Wolf Optimization (GWO), Logique Floue, MATLAB/Simulink, Systèmes de Conversion de l'Énergie Éolienne.

<u>Content</u>

Content

Chapter I: Wind Energy Conversion System Based on a Permanent Magnet Synchronous Machine (PMSM).

Chapter II: Modeling and Simulation of a Wind Turbine Based on a Permanent Magnet Synchronous Generator (PMSG).

Chapter III: Control of PMSG Using Field-Oriented Control (FOC) and PI Controllers.

Chapter IV: Grey Wolf Optimization and Fuzzy Logic- Based Control.

List of figures

List of figures

Chapter I: Wind Energy Conversion System Based on a Permanent Magnet Synchronous Machine (PMSM).

Chapter II: Modeling and Simulation of a Wind Turbine Based on a Permanent Magnet Synchronous Generator (PMSG).

Chapter III: Control of PMSG Using Field-Oriented Control (FOC) and PI Controllers.

Chapter IV: Grey Wolf Optimization and Fuzzy Logic- Based Control.

Index of Notations

Index of Notations

Symbol	Description	Unit
(V_a, V_b, V_c)	Stator phase voltages	V
(I_a, I_b, I_c)	Stator phase currents	A
(V_d, V_q)	Direct and quadrature axis voltages	V
(I_d, I_q)	Direct and quadrature axis currents	A
(R_s)	Stator resistance	Ω
(L_d)	Direct-axis inductance	H
(L_q)	Quadrature-axis inductance	H
(φ_d)	Flux linkage along d-axis	Wb
(φ_q)	Flux linkage along q-axis	Wb
(φ_f)	Permanent magnet flux linkage	Wb
(T_e)	Electromagnetic torque	N·m
(T_m)	Mechanical torque	N·m
(T_L)	Load torque	N·m
(J)	Moment of inertia	$kg{\cdot}m^2$
(f)	Viscous friction coefficient	N·m·s/rad
(ω_m)	Mechanical angular speed	rad/s
(ω_e)	Electrical angular speed	rad/s
(P)	Number of pole pairs	–
(θ_e)	Electrical rotor angle	rad
(P_e)	Electrical power	W
(P_m)	Mechanical power	W
(P_{em})	Electromagnetic power	W

Symbol	**Description**	**Unit**
(λ)	Tip-speed ratio	–
(β)	Blade pitch angle	°
(C_p)	Power coefficient	–
(P_{wind})	Available wind power	W
(P_{aero})	Aerodynamic power	W
(T_{aero})	Aerodynamic torque	N·m
(V_w)	Wind speed	m/s
(R)	Turbine blade radius	m
(S)	Swept area of turbine	m^2
(ρ)	Air density	kg/m^3
(k)	Gearbox ratio	–
(f_e)	Electrical frequency	Hz
(n)	Rotor speed	rpm
(V_{dc})	DC bus voltage	V

Abbreviation

Abbreviation

Abbreviation	Meaning
PMSM	Permanent Magnet Synchronous Machine
PMSG	Permanent Magnet Synchronous Generator
FOC	Field Oriented Control
PI	Proportional Integral
GWO	Grey Wolf Optimization
FL	Fuzzy Logic
PWM	Pulse Width Modulation
AC	Alternating Current
DC	Direct Current
MPPT	Maximum Power Point Tracking
dq	Direct-Quadrature Reference Frame

General Introduction

General Introduction

In recent decades, the world has witnessed a continuous increase in the demand for electrical energy due to population growth and rapid industrial and technological development. The excessive dependence on conventional energy sources such as oil, natural gas, and coal has led to several economic and environmental challenges, most notably the depletion of fossil fuel resources and the increase in greenhouse gas emissions. Consequently, the search for clean and renewable energy sources has become a necessity to achieve sustainable development and ensure energy security for future generations.

Renewable energy is considered one of the most promising alternatives capable of meeting the growing energy demand while reducing environmental impacts. Among the various renewable energy sources, wind energy occupies a prominent position due to its wide availability, relatively low operating costs, and the significant technological advancements achieved in wind energy conversion systems over recent years.

A wind energy conversion system consists of several interconnected components, including the wind turbine, the electrical generator, power electronic converters, and control systems. Among the different types of generators used in modern wind turbines, the Permanent Magnet Synchronous Generator (PMSG) has gained considerable attention because of its high efficiency, high power density, excellent reliability, and its ability to operate under variable-speed conditions without requiring an external excitation system.

The performance of wind energy conversion systems depends not only on the characteristics of the generator but also on the effectiveness of the applied control strategies. Among the most widely adopted techniques is Field-Oriented Control (FOC), which enables the independent control of magnetic flux and electromagnetic torque, resulting in improved dynamic response and enhanced control accuracy. Furthermore, the use of PI controllers within the control loops contributes to system stability and minimizes the error between reference and actual values.

With the continuous advancement of artificial intelligence and optimization techniques, several intelligent algorithms have been developed to improve the performance of control systems. Among these techniques, Grey Wolf Optimization (GWO) and Fuzzy Logic have demonstrated their effectiveness in enhancing control quality and increasing system efficiency through optimal parameter tuning and adaptation to varying operating conditions.

Within this context, the objective of this work is to study and model a wind energy conversion system based on a Permanent Magnet Synchronous Generator (PMSG).

Chapter I

Wind Energy Conversion System Based on a Permanent Magnet Synchronous Machine (PMSM)

I.1 Introduction:

Synchronous machines represent fundamental electrical components within contemporary industrial frameworks, largely attributed to their high operational efficiency and their inherent capacity to maintain a constant speed precisely synchronized with the power supply frequency. Distinctions among these machines primarily derive from the specific excitation methodologies employed. Among these, the permanent magnet synchronous motor (PMSM) is particularly distinguished by its superior operational characteristics, high power density, and compact structural design. These combined attributes position synchronous machines as critical elements across numerous advanced industrial and technological systems, notably encompassing applications in wind energy generation.

This chapter is dedicated to a comprehensive examination of synchronous machines, with a pronounced emphasis on the permanent magnet synchronous motor (PMSM). Initially, it delineates the historical trajectory, fundamental operating principles, internal structure, and primary application domains of the PMSM. Furthermore, it proceeds to discuss a range of control strategies, encompassing both established classical methodologies and contemporary optimization-based control approaches.

Ⅰ.2 Wind Energy System

I.2.1 General about Wind Energy

Wind energy refers to the kinetic energy of air movement, the motive force of which can be harnessed for the propulsion of sailboats and other vehicles. Alternatively, this kinetic energy can be converted into various usable forms by means of an aerogenerator, such as a wind turbine or a traditional windmill. It is recognized as a significant form of renewable energy.

The utilization of wind energy primarily encompasses three distinct applications.

Firstly, it involves the direct harnessing of mechanical energy, where wind propels vehicles such as sailing vessels or land yachts. This mechanical force is also employed for water management, exemplified by historic Majorcan mills, or for operating pumping wind turbines used in irrigation and livestock watering, and for the rotation of millstones.

Secondly, wind energy can be transformed into a motive force, serving purposes such as the pumping of liquids or the compression of various fluids.

Thirdly, it is extensively used for electrical energy generation; here, a wind turbine is mechanically coupled with an electrical generator to produce either direct current (DC) or alternating current (AC). The electrical output from such a generator can be integrated into an existing electrical grid or can operate within an autonomous system, which often incorporates a supplementary power source, such as a genset, and/or an energy storage unit, typically a battery bank or another form of energy storage technology. [1]

I.2.2 Wind Energy System components

A wind turbine comprises several intricate subsystems that collectively function to transform the mechanical energy of wind into electrical energy. Although each component is designed with specific functionalities, their synergistic integration results in a cohesive system engineered for electricity generation. [2]

Generally, wind turbines are composed of four principal sections:

- The Rotor Blades
- The Nacelle
- The Generator Assembly
- The Tower

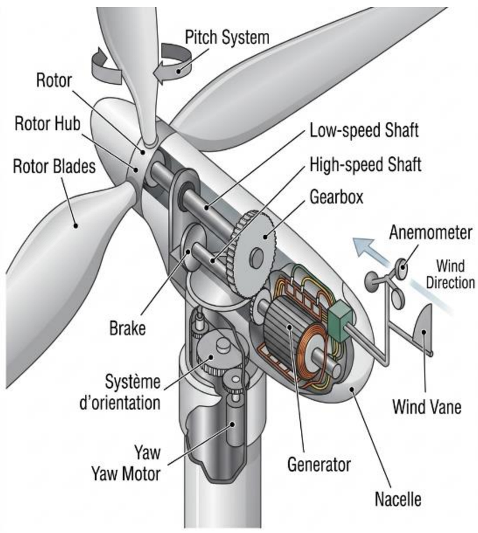

Figure I.1. Components of a Wind Turbine.

I.2.3 Operating principle

Using a device referred to as a wind turbine Figure I.1, or windmill, wind energy is converted from a kinetic form into mechanical power transmitted via a drive shaft. This mechanical power is then converted into electrical power by coupling the shaft to an electric generator. The resulting alternating current is subsequently processed by static power converters—typically rectified to direct current and, when required, inverted back to alternating current—so that it can either charge batteries or be fed directly into the grid. In this configuration, the system is commonly termed an aerogenerator. [3]

I.2.4 State of the Art on Electromechanical Conversion

The wind turbine converts the wind's kinetic energy into mechanical power. A gearbox is commonly used to adapt the turbine's rotational speed (approximately 10–200 rpm) to the operating range of conventional generators (typically 750–3000 rpm). The generator then converts the mechanical input into electrical energy, after which the generated power may be interfaced with the electrical grid either through a direct or an indirect connection.

Under direct grid connection, the generator typically operates at a fixed or nearly fixed speed, which is commonly realized by controlling the slip of an asynchronous machine. By contrast, in an indirect connection, power converters placed between the generator and the grid decouple the machine's rotational speed from the grid frequency. This arrangement enables variable-speed operation and allows the use of synchronous machines, asynchronous machines, or other specialized machine types, with the aim of improving overall system energy efficiency. [2]

Variable-speed operation can also improve the quality of the generated electrical power, as it provides additional flexibility in responding to abrupt changes in wind speed. Within this framework, variable-speed wind turbines employing Permanent Magnet Synchronous Generators (PMSG) have attracted increasing interest in recent years among wind turbine manufacturers.[11]

Because permanent magnets in the rotor provide the excitation flux, a stator magnetizing current is not required to maintain a constant air-gap flux; consequently, the stator current is primarily allocated to torque production [4]. Accordingly, for a given output power, a PMSG can achieve a higher power factor and typically exhibits higher efficiency than induction generators used in other wind-turbine configurations.

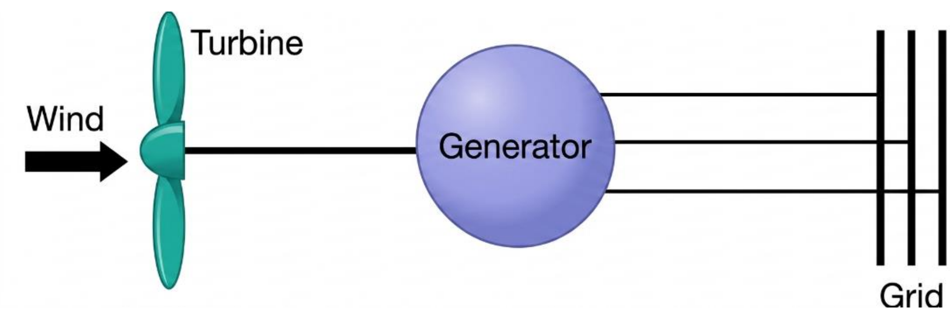

Figure I.2. Wind Turbine with a Permanent.

I.3 Permanent magnet synchronous machine

Focusing on this category of synchronous machines. Permanent magnet synchronous machines (PMSM) are high-efficiency AC motors, as they use strong magnets in the rotor instead of conventional excitation windings, which contributes to eliminating copper losses, providing high torque, and a compact size. The late eighties marked the beginning of the era of brushless permanent magnet motors, driven by the development of power electronics and rare earth magnets with high energy density. It has developed as a more efficient and reliable alternative to traditional induction motors, especially with the need for low-carbon green technologies. [5]

Figure I.3. Permanent magnet synchronous machine.

Among the most important characteristics of permanent magnet synchronous machines (PMSM).

- High efficiency and high torque: provides power equivalent to two to four times that of induction motors of the same size.
- Precise control: allows precise control of speed and position.
- High power density: excellent torque-to-weight ratio.
- No need excitation coils: the permanent magnet self-generates the magnetic field, which reduces the Heat lost and improves the efficiency (energy saving).
- Low maintenance: due to the absence of brushes and commutators.

I.3.1 Components of (PMSM)

Like any motor, synchronous machines with permanent magnets consist mainly of a fixed part (stator) and a rotating part (rotor), as well as other accessories

I.3.1.1 Stator

The stator of a permanent magnet synchronous machine resembles that of an asynchronous machine. It is composed of stacked magnetic sheets, which feature slots housing three identical windings spaced 2π/3 apart.

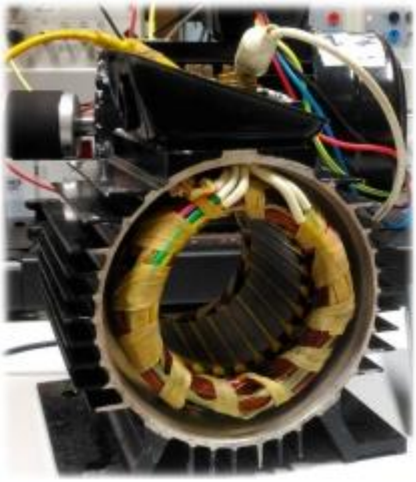

Figure I.4. Stator of machine PMSM

I.3.1.2 Rotor

The rotor in a Surface-Mounted Permanent Magnet Synchronous Machine (SMPMSM) typically comes in two forms:

- A rotor that has pole pieces. These focus the magnetic flux, and the magnets are arranged either parallel or perpendicular to the air gap, or in a more complex way. In this machine type, the inductor has jn
- A rotor without pole pieces, so it has a constant air gap where the magnets' magnetization is commonly perpendicular to the air gap.

Figure I.5. Rotor of machine PMSM.

I.3.2 Operating Principle of (PMSM)

The operational foundation of a permanent magnet synchronous motor rests on the interplay between the rotor's permanent magnetic field and the stator's electromagnetic field. When alternating current flows through the stator windings, it creates a rotating magnetic field. The rotor's permanent magnets interact with this rotating field, leading to attraction and rotation of the rotor. The rotor spins at precisely the same speed as the stator's magnetic field. There isn't any slip between them, which explains why it is called synchronous [6].

A permanent magnet synchronous motor turns electrical energy into mechanical energy. It does this by using the forces made when two magnetic fields interact. One of these fields comes from permanent magnets on the rotor (the part that turns), and the other comes from the stator (the stationary part), which makes a rotating magnetic field when electricity passes through it [7]. Where the details of its mechanism of action are as follows

Creating the Rotating Magnetic Field: The stator has coils of wire. When alternating current (AC) goes through these coils, it makes a magnetic field. This field does not stay in one place; it rotates around the stator. The speed at which it rotates depends on the frequency of the AC power.

Rotor's Role: The rotor has permanent magnets fixed to it. These magnets create their own magnetic field.

Interaction and Rotation: The magnetic field from the stator interacts with the magnetic field from the rotor's permanent magnets. Opposite poles attract, and like poles repel. This interaction makes a force that turns the rotor.

Synchronous Speed: What makes this motor synchronous is that the rotor turns at the exact same speed as the stator's rotating magnetic field. In other words, they are in sync. Unlike other types of motors. There is no slip, where the rotor turns slower than the magnetic field.

No Slip: Slip refers to the difference in speed between the rotating magnetic field and the rotor's speed. In induction motors, the rotor always turns a bit slower than the magnetic field, which allows for torque production. But in a synchronous motor, since the rotor is locked to the magnetic field because of the permanent magnets, there is no slip.[11]

In short, a permanent magnet synchronous motor works because the permanent magnets on the rotor try to catch up and align with the rotating magnetic field made by the stator. Because of this direct link, the motor provides accurate speed control and efficient turning of energy.

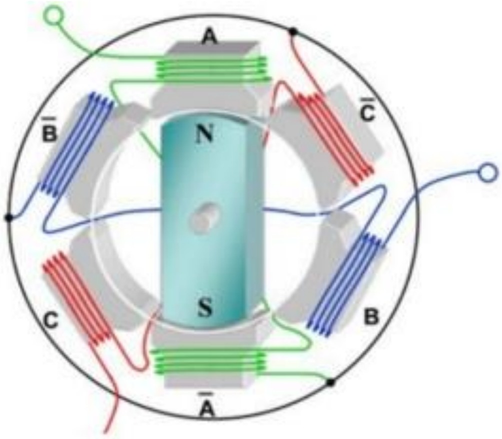

Figure I.6. Schematic Diagram of machine (PMSM).

I.3.3 Uses of the permanent magnet synchronous machine (PMSM)

Permanent magnet synchronous machines (PMSM) are one of the most widely used electrical machines in industrial and other applications due to their high efficiency, high power density, fast dynamic response, as well as accurate speed and torque control. The development of power electronics and digital control technologies has contributed to the expansion of their use to many advanced industrial and technological fields.[5] They are widely used in industrial automation and robotics applications, and are also the preferred choice in electric and hybrid vehicle propulsion systems due to their high performance and energy efficiency. They are also used as generators in renewable energy systems, due to their ability to work efficiently at low rotational speeds. These machines also find important applications in the fields of aviation, marine systems, and modern household appliances with inverter technology, where they contribute to improving performance and reducing energy consumption.

- Industrial applications and robotics: it is widely used in automation systems and precision robots due to its high efficiency in controlling speed and torque accurately .
- Electric and hybrid cars: they are considered the optimal choice in driving electric vehicles due to their high energy density, high efficiency, and compact size, which contributes to energy saving.
- Centrifuge systems and pumps: used in applications that require high speeds and stable torque such as medical and industrial centrifuges.

- Aviation and defense: used in flight control systems, mechanical actuators (Actuators) for their light weight, accuracy and reliability.
- Household appliances and air conditioning: it is used in the manufacture of compressors in modern air conditioners (inverters) and refrigerators for their energy efficiency.
- Generation and renewable energy systems: used as generators in small and medium-sized wind turbines, they provide excellent performance at low rotational speeds.

I.4 Modeling of the permanent magnet synchronous machine

I.4.1 Description

Synchronous machines with respect to asynchronous machines have a greater power by weight. Since the rotor flow is known, it is easier to control the torque.

The progress made in the manufacture of magnets, whether based on metal alloys or rare earths, means that today the use of PMSM is increasing [6].

The permanent magnet synchronous machine (PMSM) represented by **Figure I.3** comprises a stator and a rotor of symmetrical constitution with a pair of poles. In notches regularly distributed on the internal surface of the stator are housed three identical windings, their axes are spaced apart from each other by an electrical angle equal to ($2\pi/3$) and connected in a star with isolated neutral.

I.4.2 Problems of modeling

The unified theory of classical electrical machines, also called generalized theory, is based on the Park transformation which relates the stator and rotor electrical equations to the electrically perpendicular axes called d, for direct, and q for quadrature. These two axes are used, for example in Blondel's theory of synchronous machines and linked to the rotor. The d axis is the polar axis and the q axis is the interpolar axis [6].

The modeling of machines and converters in dynamic mode is also a mandatory passage, whether in continuous models with transfer functions or correcting equations or the determination of numerical control calculation algorithms.

The model of alternating current machines is much more complex than that of direct current machines and their control will be more complex, due to the fact that [12],[6]:

- All the quantities are alternating, fixed or variable frequency.

- But The degree of the electromechanical system is usually higher than that of systems based on direct current machines.
- In the systems and nonlinear with variable coefficients and multiple inputs and outputs.
- There can be four types of synchronous machine :
- A synchronous machine with a wound rotor and a smooth air gap ($Ld = Lq$).
- Synchronous machine with wound rotor and protruding pole ($Ld > Lq$), (effect of salience, increase in max torque).
- A synchronous machine with permanent magnets mounted on the surface of the rotor without pole pieces ($Ld = Lq$), (large air gap, we can have a trapezoidal torque),
- Synchronous machine parts buried in the rotor, ($Ld < Lq$), (possibility of high rotation speeds).

For our case, we are interested in the study, modeling and control of the latest variant of the synchronous machines mentioned above.

I.4.3 Simplifying assumptions

The electrical and dynamic behavior of electrical machines can only be studied if it is defined by a mathematical model. To obtain this model, the following simplifying assumptions are taken into account [7],[5],[13]:

However, the air gap is of uniform thickness, and of negligible notching.

During the saturation of the magnetic circuit, the hysteresis and the eddy currents are negligible.

However, the resistances of the windings do not vary with the temperature and the skin effect is negligible.

Thus, it is assumed that the FMM created by each of the phases of the two armatures is sinusoidally distributed.

I.4.4 Characteristic of the PMSM

A synchronous machine with a rare earth permanent magnet, which generates a constant excitation flow to the rotor (φ_f).

The machine is not equipped with a shock absorber.

All the magnets are buried in the rotor with an inverted salience, therefore the natural inductances of the stator along the axes d and q are different ($L_d > L_q$) [6].

I.5 Putting the synchronous machine into an equation

To establish simple relationships between the motor supply voltages and these currents, we consider the following ideal synchronous machine model.

I .5.1 Choice of the Repository

The Park reference frame (d,q) linked to the rotor [12],[14] is chosen.

Where ω is the pulsation of the stator quantities in the system (d,q).

I.5.2 Model of the PMSM in the Park repository

The Park transformation brings the stator equations back into a frame of reference linked to the rotor. So the equivalent machine is identical to a direct current machine having the winding f as an inductor and having two quadrature armatures. [15],[9]

I.5.3 Equations of the PMSM

I.5.3.1 Stator Voltage Equations

For a three-phase PMSM, the stator voltage equations in phase variables are derived from Kirchhoff's voltage law.

For each phase:

$$v_a = R_s i_a + \frac{d\varphi_a}{dt} \quad \text{(I.1)}$$

$$v_b = R_s i_b + \frac{d\varphi_b}{dt} \quad \text{(I.2)}$$

$$v_c = R_s i_c + \frac{d\varphi_c}{dt} \quad \text{(I.3)}$$

Where:

- v_a, v_b, v_c are stator phase voltages
- i_a, i_b, i_c are stator phase currents
- R_s is stator resistance
- $\varphi_a, \varphi_b, \varphi_c$ are stator flux linkages

In matrix form:

$$\mathbf{v}_{abc} = R_s \mathbf{i}_{abc} + \frac{d}{dt}\boldsymbol{\varphi}_{abc} \quad \text{(I.4)}$$

I.5.4 Flux Linkage Expressions

The stator flux linkage consists of two components:

1. Self and mutual inductance flux
2. Rotor permanent magnet flux

Thus:

$$\varphi_{abc} = \mathrm{L}_{abc}\mathrm{i}_{abc} + \varphi_{pm} \tag{I.5}$$

Where:

- $\mathbf{L}_{abc}$ is the inductance matrix
- $\boldsymbol{\varphi}_{pm}$ is rotor permanent magnet flux vector

For a symmetric three-phase machine:

$$\mathbf{L}_{abc} = \begin{bmatrix} L_s & M & M \\ M & L_s & M \\ M & M & L_s \end{bmatrix} \tag{I.6}$$

Where:

- L_s= self inductance
- M= mutual inductance

I.5.5 Permanent Magnet Flux in abc Frame

The rotor magnet flux depends on rotor electrical position θ_e.

$$\varphi_{pm,a} = \varphi_f \cos(\theta_e) \tag{I.7}$$

$$\varphi_{pm,b} = \varphi_f \cos\left(\theta_e - \frac{2\pi}{3}\right) \tag{I.8}$$

$$\varphi_{pm,c} = \varphi_f \cos\left(\theta_e + \frac{2\pi}{3}\right) \tag{I.9}$$

Where:

- φ_f= permanent magnet flux linkage
- $\theta_e = p\theta_m$(electrical angle)
- p= number of pole pairs

I.5.6 Complete Voltage Equation

Substituting flux into voltage equation:

$$\mathbf{v}_{abc} = R_s \mathbf{i}_{abc} + \mathbf{L}_{abc} \frac{d\mathbf{i}_{abc}}{dt} + \frac{d\boldsymbol{\varphi}_{pm}}{dt} \tag{I.10}$$

This represents the complete stator electrical model in the natural frame.

I.6 Clarke Transformation (abc → αβ)

To simplify the model, we apply Clarke transformation.

$$\begin{bmatrix} i_\alpha \\ i_\beta \end{bmatrix} = \frac{2}{3} \begin{bmatrix} 1 & -\frac{1}{2} & -\frac{1}{2} \\ 0 & \frac{\sqrt{3}}{2} & -\frac{\sqrt{3}}{2} \end{bmatrix} \begin{bmatrix} i_a \\ i_b \\ i_c \end{bmatrix} \tag{I.11}$$

Similarly for voltages and fluxes.

This converts the three-phase system into two orthogonal stationary components.

I.7 Park Transformation (αβ → dq)

The rotating reference frame is defined by angle θ_e.

$$\begin{bmatrix} i_d \\ i_q \end{bmatrix} = \begin{bmatrix} \cos\theta_e & \sin\theta_e \\ -\sin\theta_e & \cos\theta_e \end{bmatrix} \begin{bmatrix} i_\alpha \\ i_\beta \end{bmatrix} \tag{I.12}$$

This transformation eliminates time-varying inductances.

I.8 PMSM Model in dq Reference Frame

After transformation, voltage equations become:

$$v_d = R_s i_d + L_d \frac{di_d}{dt} - \omega_e L_q i_q \tag{I.13}$$

$$v_q = R_s i_q + L_q \frac{di_q}{dt} + \omega_e L_d i_d + \omega_e \lambda_f \tag{I.14}$$

Where:

- L_d, L_q= dq inductances
- $\omega_e = p\omega_m$

I.9 Electromagnetic Torque Derivation

The electromagnetic torque is derived from co-energy:

Substituting flux:

$$\varphi_d = L_d i_d + \varphi_f \tag{I.15}$$

$$\varphi_q = L_q i_q \tag{I.16}$$

Thus:

$$T_e = \frac{3}{2} p\left[\varphi_f i_q + (L_d - L_q) i_d i_q\right] \quad (I.17)$$

For Surface PMSM:

$$L_d = L_q$$

Then torque simplifies to:

$$T_e = \frac{3}{2} p \varphi_f i_q$$

I.10 Mechanical Model

Using Newton's second law for rotation:

$$J\frac{d\omega_m}{dt} = T_e - T_L - B\omega_m \quad (I.19)$$

Where:

- J= moment of inertia
- B= friction coefficient
- T_L= load torque

Electrical and mechanical speeds are related by:

$$\omega_e = p\omega_m \quad (I.20)$$

I.11 Complete State-Space Model

The state variables are:

$$x = [i_d, i_q, \omega_m]^T \quad (I.21)$$

Electrical equations:

$$\frac{di_d}{dt} = \frac{1}{L_d}(v_d - R_s i_d + \omega_e L_q i_q) \quad (I.22)$$

$$\frac{di_q}{dt} = \frac{1}{L_q}(v_q - R_s i_q - \omega_e L_d i_d - \omega_e \lambda_f) \quad (I.23)$$

Mechanical equation:

$$\frac{d\omega_m}{dt} = \frac{1}{J}(T_e - T_L - B\omega_m) \quad (I.24)$$

These last equations constitute the basis of the block diagram of the PMSM.

The frequency of the currents at the stator is controlled by the rotation of the rotor so as to maintain synchronism between the field created by the stator currents and the magnetic moment of the rotor. It follows from this that the stator field "rotates" at the speed of the rotor. When the rotor stops, the stator field is stationary; this is the principle of autopilot

I.12 Simulation results

The purpose of this simulation was to determine the dynamic characteristics and functionality of the Permanent Magnet Synchronous Machine (PMSM). In particular, the simulation focused on the rotor (speed), electromagnetic (torque) and stator (currents) measurements taken within the dq reference frame during both steady state and transient states. The simulation time was capped at ten seconds for a clear analysis of machine response, stability, and regulation capability.

The PMSM model used in the simulation was defined with these parameters: stator resistance $Rs = 0.6\,\Omega$; direct axis inductor $Ld = 1.4 \times 10^{-3}\,H$; quadrature axis inductor $Lq = 2.8 \times 10^{-3}\,H$; number of pole pairs $P = 4$; inertia constant $J = 0.02\,Kg.m^2$; and viscous friction constant $f = 0.0014\,N.m.s$. These parameters were chosen to provide a realistic operating environment while still providing an accurate dynamic representation of the machine.

Results from simulations indicate that the PMSM has demonstrated excellent dynamic performance and steady-state operation under the adopted control action. The rotor speed achieves its reference value quickly with very little oscillation and virtually no steady-state error, demonstrating that the regulation is accomplished quickly and effectively. The electromagnetic torque is initially at a very high value to overcome rotor inertia and subsequently levels off smoothly after completion of the transient period. The stator currents in the dq reference frame show abrupt transients during startup, but eventually converge to steady-state values thereby demonstrating that the control action produces effective results. The Iq component is primarily responsible for torque production while the Id component is responsible for regulating magnet

flux. Overall, these results indicate that the PMSM model is reliable and effective as implemented in the MATLAB/Simulink environment.

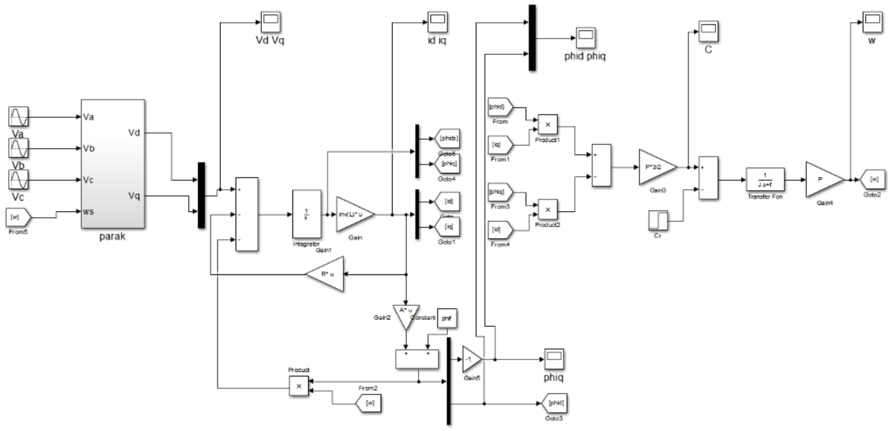

Figure I.7. Block diagram of simulating the PMSM.

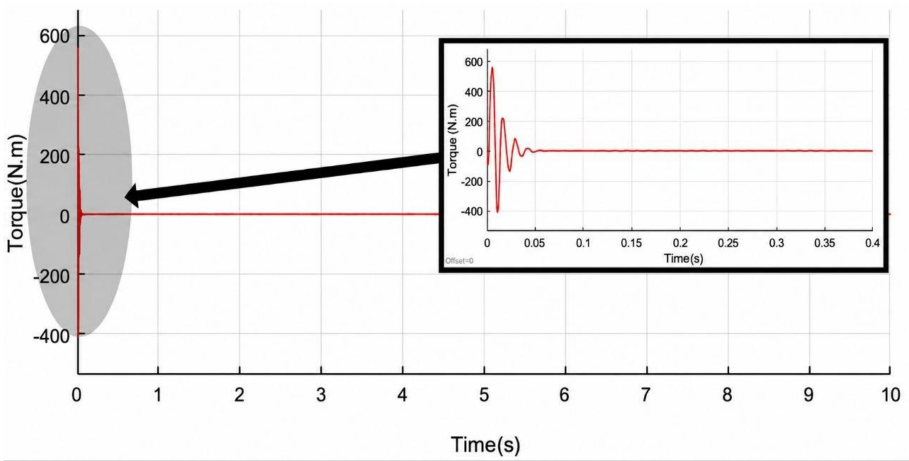

Figure I.8. Simulation results of Torque.

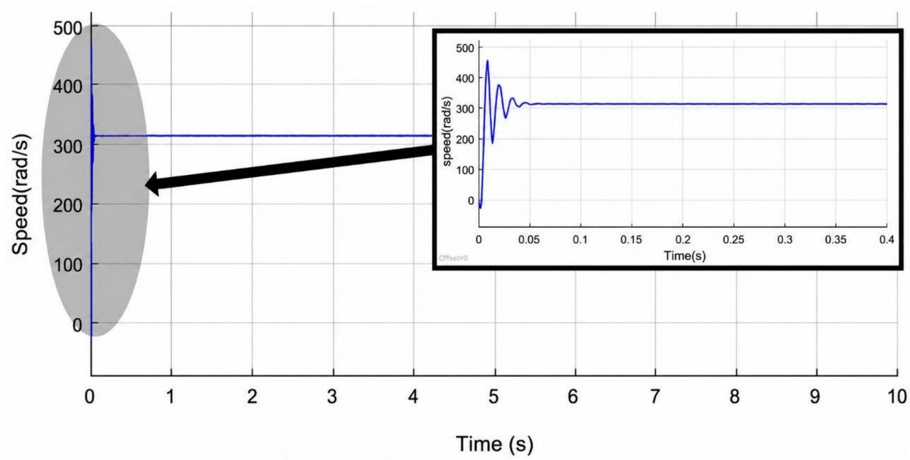

Figure I.9. Simulation results of speed.

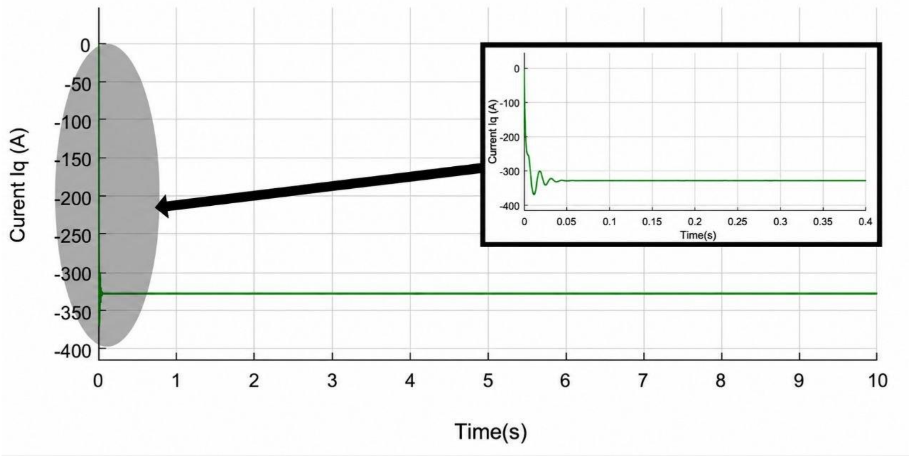

Figure I.10. Simulation results of current Iq.

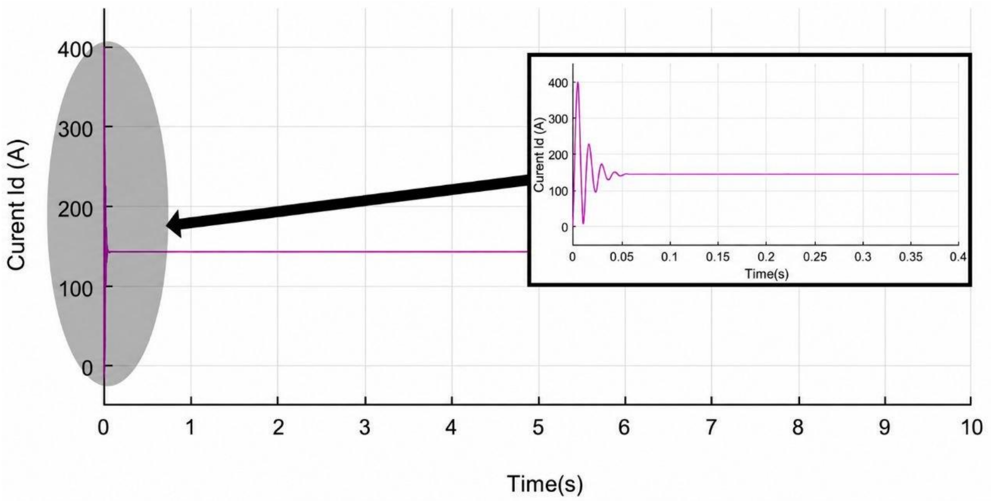

Figure I.11. Simulation results of current Id.

I.13 Conclusion

The modeling of the Permanent Magnet Synchronous Machine (PMSM) was presented in this chapter, with particular emphasis on the electrical and mechanical equations governing the dynamic behavior of the machine.

The next chapter will focus on the study and modeling of the Permanent Magnet Synchronous Generator (PMSG) based on the PMSM model, as well as the study and modeling of the wind turbine and its integration with a grid-connected generator.

Chapter II

Modeling and Simulation of a Wind Turbine Based on a Permanent Magnet Synchronous Generator (PMSG).

II.1. Introduction

The expanding deployment of electrical machines across diverse application domains has contributed to rising energy demand within industrial sectors. Alternators based on synchronous machines remain a principal means of electrical energy generation. When coupled to hydraulic, steam, or wind turbines, these units rank among the largest energy-conversion systems in current use.

In Permanent Magnet Synchronous Machines (PMSMs), permanent magnets replace the conventional field winding. The resulting excitation field removes the need for brushes and tends to reduce rotor losses, which in turn supports improved reliability and efficiency. PMSMs are therefore used in a broad range of settings, including machine tools, robotics, aerospace generation, and electric traction.

The analysis and control of these machines generally depend on an accurate mathematical model that represents key parameters such as resistance and inductance. Such a model supports examination of the physical phenomena that arise during operation and helps address technical challenges encountered in practice [19].

This chapter initially outlines the primary structural elements of the machine, subsequently establishing the mathematical model for the Permanent Magnet Synchronous Generator (PMSG) across both the rotor and stator (Park) reference frames. Furthermore, the operational characteristics of the system under grid-connected conditions are examined.

II.2 Modeling of the Permanent Magnet Synchronous Generator (PMSG)

II.2.1 Description

An alternator comprises two primary constituents: a stationary component and a rotating component. The stator, also known as the armature, is constructed from a laminated core that typically assumes the form of a hollow cylinder. This core incorporates slots designed to house the conductors of a three-phase winding, configured for 2p poles. The coils constituting this winding are electrically phase-shifted by $\left(\frac{2\pi}{3}\right)$ radians. They are invariably connected in a star (or wye) configuration, with the neutral point made accessible primarily for grounding purposes.

The rotor, which functions as the field system, integrates **p** north poles and **p** south poles, positioned in an alternating sequence. These poles are generated either through field windings energized by a direct current source or by employing permanent magnets. Structurally, rotors can be categorized into salient-pole or non-salient (smooth) designs, as detailed in references [17].

The quantity of poles within an alternator is fundamentally defined by the rotational speed of the rotor and the frequency of the electrical current it generates. To illustrate this relationship, let us consider a conductor situated within the stator, past which the alternating north and south poles of the rotor traverse. Should the induced voltage in this conductor exhibit a series of positive excursions during the transit of a north pole, it will correspondingly manifest equal yet negative values upon the subsequent passage of a south pole. Consequently, each complete traversal of a pole pair across a stator conductor correlates with the completion of one full cycle of the induced voltage. This implies that the resultant frequency can be expressed by the ensuing equation:

$$f = \frac{p.n}{120} \tag{II.1}$$

II.2.2. Operating Principle of a Synchronous Generator (PMSG)

Within a synchronous generator, the mechanically actuated rotor's field system generates a magnetic field that varies spatially across the stator windings. The electromotive forces (EMFs) induced as a consequence in these windings initiate currents, which then collectively establish a stator magnetic field within the air gap. This stator field is observed to rotate at a speed identical to that of the rotor's magnetic field [17].

The fundamental operating principle revolves around the dynamic interaction initiated by the rotation of a magnet, termed the rotor. As this rotor passes in proximity to the fixed faces of three coils, collectively referred to as the stator and connected to the electrical network, a variation in magnetic flux is generated. This temporal fluctuation in magnetic flux consequently induces an electromotive force within each individual coil, ultimately leading to the generation of a three-phase current.

II.2.3. Modeling of the Permanent Magnet Synchronous Generator

Similar to other three-phase electrical machines, this particular generator incorporates a wound stator. A distinguishing characteristic of the Permanent Magnet Synchronous Generator (PMSG), however, is the utilization of permanent magnets within its rotor assembly. This design inherently mitigates the requirement for a brush and slip-ring system, consequently decreasing rotor losses and obviating the need for an external power source to supply excitation current [22]. This arrangement, in turn, induces an electromotive force within each stator coil, thereby producing a three-phase output current.

The modeling of a Permanent Magnet Synchronous Generator (PMSG) requires the establishment of a robust mathematical framework. This framework is essential for accurately representing the inherent electromagnetic and mechanical processes that govern the machine's operation. Such an approach permits a comprehensive analysis of the system's state variables across both transient and steady-state conditions, consequently providing a reliable foundation for simulation and subsequent performance evaluation [23].

II.2.4 Simplifying Assumptions

A mathematical model for the synchronous electrical machine is commonly developed under a set of fundamental simplifying assumptions:

- Magnetic saturation within the magnetic circuit is considered negligible.
- The magnetomotive force (MMF) generated by the stator windings is posited to exhibit a sinusoidal spatial distribution.
- Hysteresis, eddy current losses, and the skin effect are typically excluded from the analysis.
- Slotting effects are similarly deemed negligible.
- The winding resistance is postulated to remain constant, showing no dependence on variations in temperature.

A Permanent Magnet Synchronous Machine (PMSG) is characterized by a three-phase winding situated in its stator, with the rotor's excitation being furnished by permanent magnets. These permanent magnets are typically modeled as rigid structures, possessing a magnetic permeability approximating that of air [21].

II.2.5 Electrical Equations of the PMSG

The electrical equations of electrical machines in a stationary reference frame linked to the stator are described by:

$$\begin{bmatrix} V_a \\ V_b \\ V_C \end{bmatrix} = [-R_s] \begin{bmatrix} i_a \\ i_b \\ i_c \end{bmatrix} + \frac{d}{dt} \begin{bmatrix} \varphi_a \\ \varphi_b \\ \varphi_c \end{bmatrix} \tag{II.2}$$

$(V_a V_b V_c)$: Stator phase voltage vector.

$(i_a i_b i_c)$: Stator phase current vector.

$(\varphi_a \varphi_b \varphi_c)$: Vector of the total flux linkages through the stator windings.

R_s : Stator phase resistance.

The stator windings of the synchronous machine under consideration are configured in a star (wye) arrangement, featuring an isolated neutral point. This design dictates that the instantaneous summation of the stator phase currents consistently yields zero, thereby preventing the manifestation of any zero-sequence current. It follows that even if zero-sequence components of voltage or flux are present within the system, they will not impart any contribution to the electromagnetic torque. Consequently, the dynamic behavior of this machine can be effectively analyzed and represented through the employment of two independent variables.

II.2.6 Transformation to the Park Reference Frame

To simplify the dynamic model of the machine, a reference frame transformation is employed. This mathematical operation effectively maps the three fixed stator windings, originally displaced

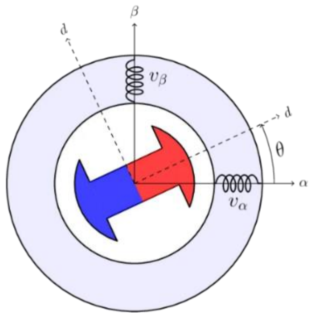

Figure II.1. Representation of (PMSG) in the Park (d, q) Reference Frame.

by (2π/3), onto a new representation comprising two fictitious equivalent windings. These transformed windings exhibit a (π/2) phase shift and are inherently aligned with the rotor's reference frame

The two d- and q-axis coils, rotating synchronously with the rotor, generate an effect comparable to that produced by the three stationary windings. Expressing system variations within this newly established (d, q) reference frame facilitates the transformation from the natural

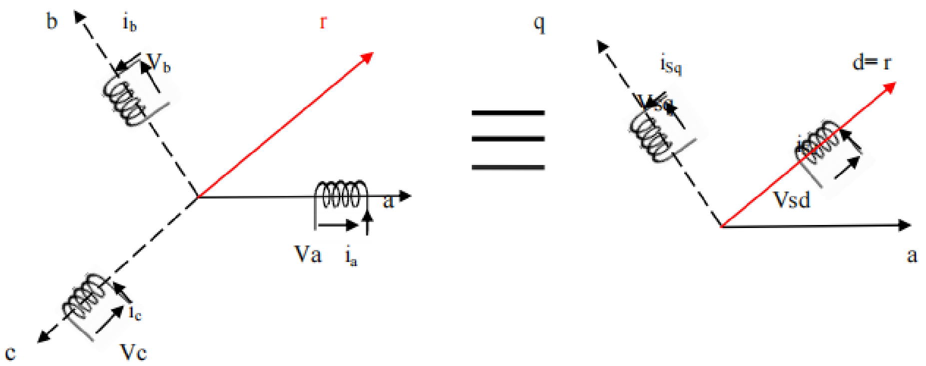

Figure II.2. Transformation from the Stator Natural Reference Frame to the Park (d,q) Reference Frame.

coordinate system to the Park reference frame, thereby yielding a relatively simplified model of the machine [21].

Using the Park transformation, the real (phase) quantities (v_a, v_b, v_c) and (i_a, i_b, i_c) are transformed into their components in the new reference frame (v_0, v_b, v_c) and (i_0, i_b, i_c).

The Park transformation matrix is expressed as follows:

$$P(\theta) = \begin{bmatrix} \cos(\theta) & \cos\left(\theta - \frac{2\pi}{3}\right) & \cos\left(\theta - \frac{4\pi}{3}\right) \\ -\sin(\theta) & -\sin\left(\theta - \frac{2\pi}{3}\right) & -\sin\left(\theta - \frac{4\pi}{3}\right) \\ \frac{1}{2} & \frac{1}{2} & \frac{1}{2} \end{bmatrix} \tag{II.3}$$

The inverse Park transformation is given by:

$$P^{-1}(\theta) = \begin{bmatrix} \cos(\theta) & -\sin(\theta) & 1 \\ \cos\left(\theta - \frac{2\pi}{3}\right) & -\sin\left(\theta - \frac{2\pi}{3}\right) & 1 \\ \cos\left(\theta - \frac{4\pi}{3}\right) & -\sin\left(\theta - \frac{4\pi}{3}\right) & 1 \end{bmatrix} \tag{II.4}$$

II.2.7 Magnetic Equations

In synchronous machines with a sinusoidal distribution of conductors, (φ_d) and (φ_q) are linear functions of the currents (i_d) and (i_q):

$$\varphi_d = L_d i_d + \varphi_f \tag{II.5}$$

$$\varphi_q = L_q i_q \tag{II.6}$$

L_d and L_q are the direct-axis and quadrature-axis inductances, respectively, and they are assumed to be independent of θ .

φ_f represents the magnetic flux produced by the permanent magnets.

By adopting the generator convention, the directions of the currents i_d and i_q are reversed within the park reference. Consequently, the derived model for the permanent magnet synchronous generator can be formulated as:

$$V_d = R_s I_d - L_d \frac{dI_d}{dt} + \omega L_q I_q \tag{II.7}$$

$$V_q = R_s I_q - L_q \frac{dI_q}{dt} - \omega L_d I_d + \omega \varphi_f \tag{II.8}$$

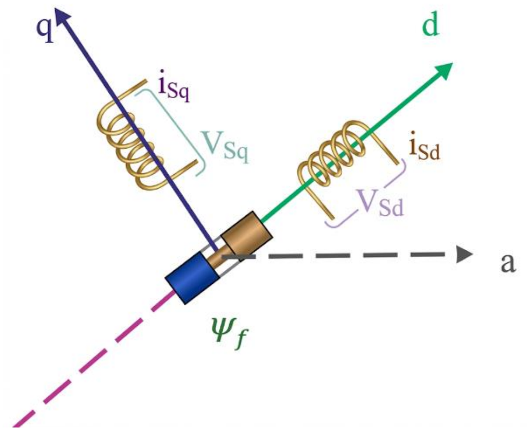

Figure II.3. Park Model of (PMSG).

II.2.8 Expression of the Electromagnetic Torque

The electromagnetic torque (C_{em}) is conventionally expressed as the partial derivative of the electromagnetic energy stored with respect to the rotor's mechanical angular position [21]:

$$C_{em} = \frac{dW_e}{d\theta_{geo}} = P\frac{dW_e}{d\theta_e} \tag{II.9}$$

W_e: Energy stored in the magnetic circuit.

θ_{geo}: Angular displacement of the moving part.

P: Number of pole pairs.

The expression of the power transmitted in the Park reference frame is given by:

$$P(t) = \frac{3}{2}\left(V_d I_d + V_q I_q\right) \tag{II.10}$$

By substituting V_d and V_q with their respective expressions, we obtain:

$$P(t) = \frac{3}{2}\left[-R_s\left(i_d^2 + i_q^2\right) + \frac{d}{dt}\left(\varphi_d i_d + \varphi_q i_q\right) + \omega\left(\varphi_d i_q - \varphi_q i_d\right)\right] \tag{II.11}$$

$\frac{3}{2} R_s\left(i_d^2 + i_q^2\right)$: Represents the power dissipated as Joule losses in the stator windings

$\frac{3}{2}\left(\varphi_d \frac{di_d}{dt} + \varphi_q \frac{di_q}{dt}\right)$: Represents the variation of the magnetic energy stored in the stator windings

$\frac{3}{2}\left(\varphi_d i_q - \varphi_q i_d\right)\frac{d\theta}{dt}$: Represents the electromagnetic power. Knowing that:

$$\omega = p\,\Omega \quad \text{and} \quad P_{em} = C_{em}\,\Omega \tag{II.12}$$

The expression of the electromagnetic torque can be written as:

$$C_{em} = \frac{3}{2}p\left(\varphi_d i_q - \varphi_q i_d\right) \tag{II.13}$$

After performing the necessary substitutions, it can be expressed as:

$$C_{em} = \frac{3}{2}p\left[\left(L_d - L_q\right)i_d i_q + \varphi_f i_q\right] \qquad \text{(II.14)}$$

II.2.9 Mechanical Equations

The dynamic equation of the PMSG is given as follows:

$$J\frac{d\Omega}{dt} = C_m - C_{em} - f\Omega \quad (II\text{-}13) \qquad \text{(II.15)}$$

Where:

- $\boldsymbol{T_m}$: Mechanical torque applied to the generator
- $\boldsymbol{T_{em}}$: Electromagnetic torque
- $\boldsymbol{f\Omega}$: Friction torque
- $\boldsymbol{J}$: Total moment of inertia of the machine
- $\boldsymbol{f}$: Viscous friction coefficient

II.2.10 Simulation results

This simulation was carried out to study the dynamic performance of a permanent magnet synchronous generator (PMSG) using specified parameters, with particular emphasis on the voltage and currents expressed in the dqreference frame over a simulation period of $20\ s$.

The results aim to characterize both the transient and steady-state behaviors of the system, as well as to evaluate its stability

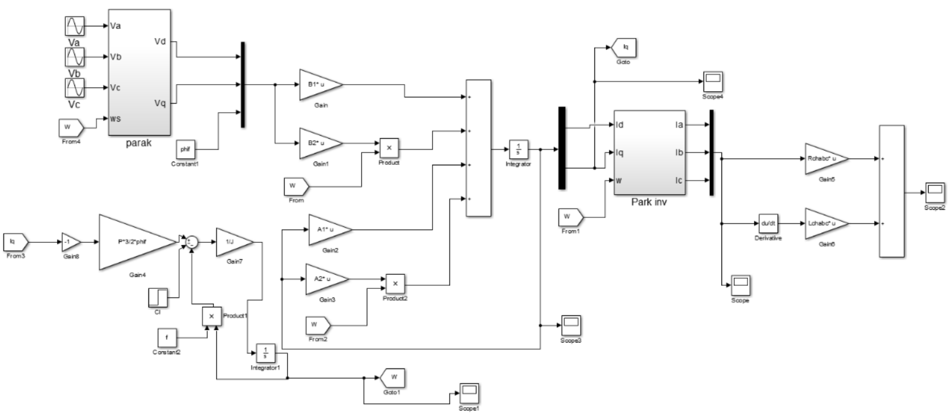

Figure II.4. MATLAB simulation of PMSG.

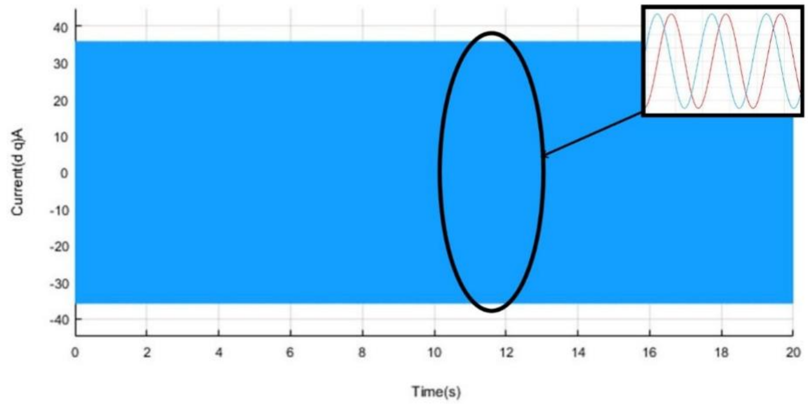

Figure II.6. Simulation results of current (d q).

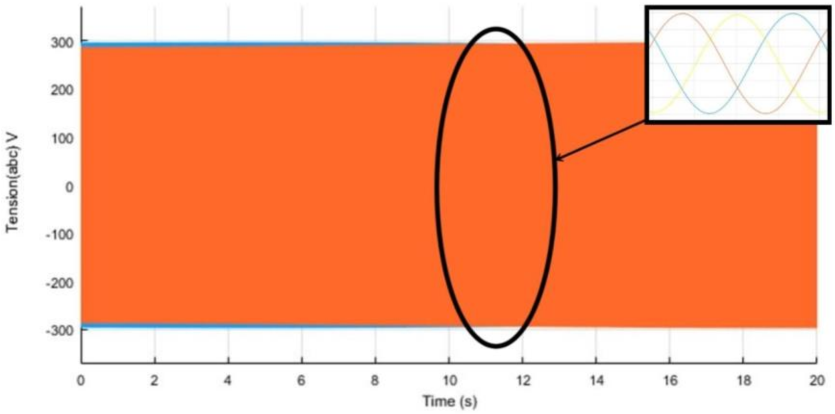

Figure II.5. Simulation results of tension(abc).

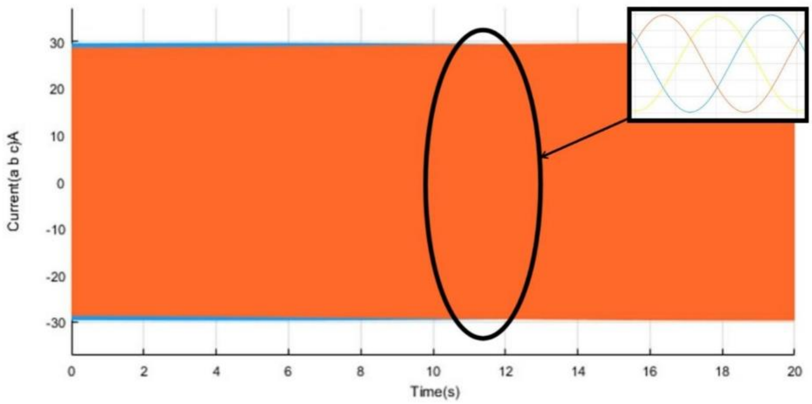

Figure II.7. Simulation results of current (a b c).

II.3 Turbine Modeling

II.3.1 Aerodynamic Torque of the Wind Turbine

Turbine modeling necessitates the development of a precise mathematical representation that quantifies the power extractable from the wind as a function of both the incident wind speed and the turbine's operational parameters, specifically its rotational velocity. This analytical approach seeks to enhance comprehension of the turbine's dynamic response across diverse operational scenarios, thereby facilitating an assessment of the system's aggregate performance. Moreover, this modeling framework permits the quantification of the aerodynamic torque exerted on the wind turbine's low-speed shaft, an aspect critical for investigating energy transfer and transformation processes inherent to the system. Consequently, the available wind power, often termed aerodynamic power, is defined thus:[1],[2]

$$P_v = \frac{1}{2}\rho S V^3 = \frac{1}{2}\rho.\pi.R^2.V^3 \tag{II.16}$$

ρ: Air density, equal to 1.22 kg/m³ at atmospheric pressure and 15°C. According to Betz's law, this power can never be fully extracted.

S: The circular area swept by the turbine; the radius of the circle is determined by the blade length R, where $S = \pi R^2$.

V: Wind speed.

In reality, the conversion device (the wind turbine) extracts an aerodynamic power $P_t$that is lower than the available power P_v.

$$\mathrm{P_t} = \frac{1}{2}\,\mathrm{C_p}(\lambda, \beta)\rho\,\pi\,\mathrm{R}^2\,\mathrm{V}^3 \tag{II.17}$$

A wind turbine can only convert a certain percentage of the power captured from the wind. This percentage is represented by $C_p(\lambda, \beta)$, which depends on the tip-speed ratio $\lambda$and the blade pitch angle β.

The power coefficient $C_p$represents the aerodynamic efficiency of the wind turbine (P_t/P_v). It depends on the turbine's characteristics. The expression of the power coefficient is interpolated in the following form:

$$\mathrm{C_p}(\lambda, \beta) = A_1\left(\frac{A_2}{\lambda_i} - A_3\beta - A_4\right)e^{-\frac{A_5}{\lambda_i}} + A_6\lambda \tag{II.18}$$

With:

$$\frac{1}{\lambda_i} = \left(\frac{1}{\lambda + 0.08\beta} - \frac{0.035}{\beta^3 + 1}\right) \quad \text{(II.19)}$$

presents the observed variation of the power coefficient (C_p) for the wind turbine examined in this thesis. The maximum power coefficient (C_{pmax}) of 0.48 is achieved when the blade pitch angle (β) is 0° and the tip-speed ratio attains its optimal value (λ_{optim}) of 8.1. To optimize power extraction, it is imperative to operate the turbine at this specific optimal tip-speed ratio, thus sustaining the power coefficient at its peak value ($C_{pmax} = 0.48$).

The turbine torque is defined as the ratio of the aerodynamic power to the turbine's rotational

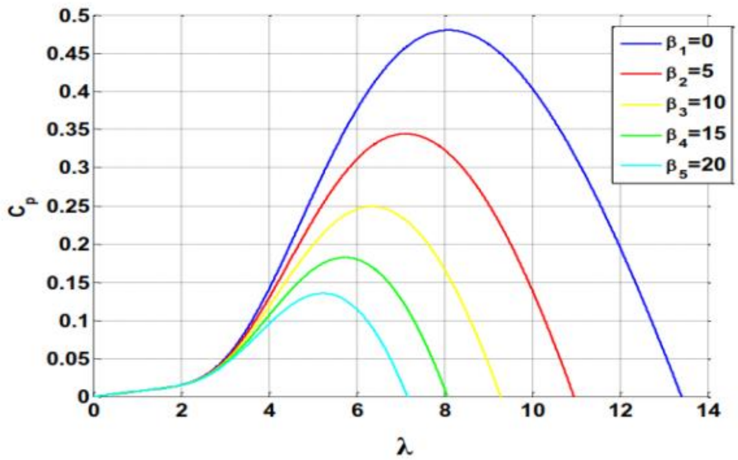

Figure II.8. Variation of the Power Coefficient as a Function of λ and β.

speed, (Ω_t).

$$T_t = \frac{1}{2}\frac{\rho\pi R^2 C_p(\lambda,\beta)V^3}{\Omega_t} \quad \text{(II.20)}$$

with $\boldsymbol{\omega_t} = \boldsymbol{\omega_m}$ since the gearbox ratio k = 1

Ω_t : Turbine speed.

T_t : Aerodynamic torque.

The tip-speed ratio (λ) is defined as the ratio between the linear speed of the blades (i.e., the turbine's rotational speed) and the wind speed.

$$\lambda = \frac{\Omega_t R}{V} \quad \text{(II.21)}$$

the power coefficient typically achieves its peak at a particular tip-speed ratio, referred to as (λ_{opt}). At this specific operational state, the power coefficient (C_p) reaches its highest point, which is indicative of the most efficient power capture from the available wind resource.[8]

Drawing upon this fundamental principle, it becomes feasible to formulate control strategies aimed at sustaining optimal power extraction across a range of wind velocities. This operational mode is upheld until the generator's rated power capacity is met; subsequently, any further power extraction is regulated and constrained to this predetermined nominal output.[2]

II.3.2 Power Maximization and Pitch Angle Control

The formulation of the control structure is predicated on the assumption that wind speed variations are negligible during steady-state operation. Given this premise, the aerodynamic torque may be precisely estimated through the combined utilization of an available wind speed estimate and the concurrently measured mechanical rotational speed.

$$T_t^* = \frac{P_{tmax}}{\omega_m^*} = \frac{1}{2\omega_m^*} C_{Pmax} \rho S V_{ref}^3 \tag{II.22}$$

Given the inherent challenges in directly measuring wind speed at the turbine level, its value is typically estimated through the application of the subsequent equation.

$$V_{ref} = \frac{\omega_m^* R}{\lambda_{opt}} \tag{II.23}$$

Additionally, to safeguard the wind energy system and ensure its stable operation, while simultaneously maintaining power output at its nominal level, pitch angle control is a frequently adopted mechanical strategy. This approach involves modifying the blade pitch angle in response to variations in wind speed. Its primary function is to regulate both the output power and rotational speed when the generator speed surpasses 30% of its rated capacity. The structural configuration of this pitch angle control system is presented in Figure II.9,[1].

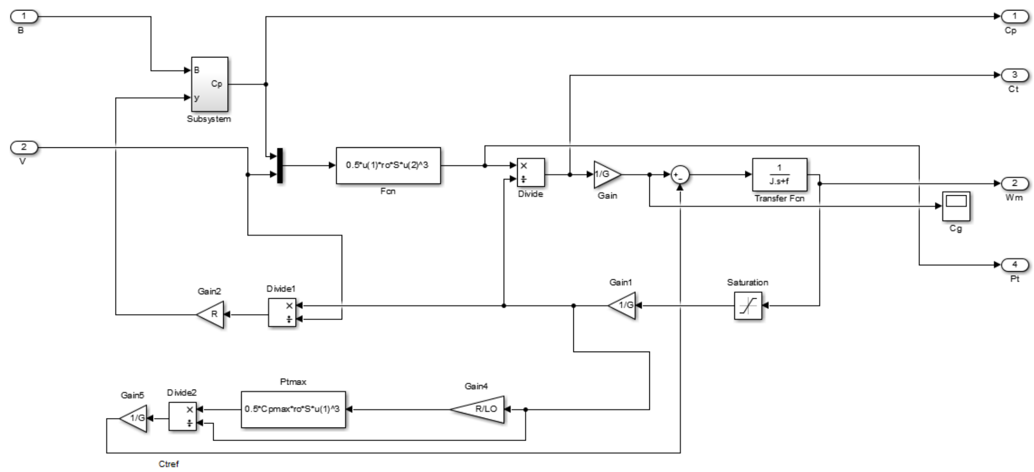

Figure II.9. MATLAB simulation of wind turbine.

II.4 Modeling of Inverter

The two-level three-phase inverter is one of the most commonly used topologies for interfacing decentralized power generation units with the electrical grid. It enables the conversion of a DC voltage V_{dc} into a three-phase AC voltage system through PWM control, which modulates the duty cycles of semiconductor switches (IGBT, MOSFET) [16].

Each inverter leg can switch between two voltage levels, either $+V_{dc}/2$ or $-V_{dc}/2$, depending on the adopted configuration (with or without a neutral point).

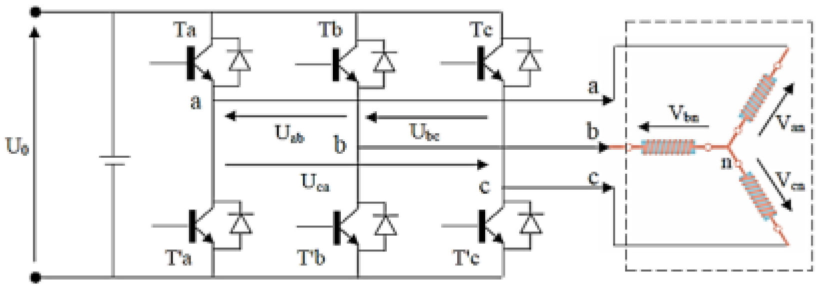

Figure II.10. Schematic Diagram of an Inverter.

The line voltages at the inverter terminals are expressed as follows:

$$\begin{cases} U_{ab} = V_{ao} + V_{bo} = V_{ao} - V_{bo} \\ U_{bc} = V_{bo} + V_{co} = V_{bo} - V_{co} \\ U_{ca} = V_{co} + V_{ao} = V_{co} - V_{ao} \end{cases} \tag{II.24}$$

U_{ab}, U_{bc}, and U_{ca} can be considered as the inverter input voltages.

The inverter equation in matrix form is represented as follows:

$$\begin{bmatrix} V_{an} \\ V_{bn} \\ V_{cn} \end{bmatrix} = \frac{u_0}{3} \begin{bmatrix} 2 & -1 & -1 \\ -1 & 2 & -1 \\ -1 & -1 & 2 \end{bmatrix} \begin{bmatrix} S_a \\ S_b \\ S_c \end{bmatrix} \tag{II.25}$$

II.5 Modeling of Rectifier

The machine-side converter plays a fundamental role in the energy conversion chain of a wind energy system based on a permanent magnet synchronous generator (PMSG). It provides the interface between the generator and the DC bus, thereby ensuring the controlled transfer of the energy produced by the turbine toward the grid-side conversion stage.

In modern high-performance systems, a PWM rectifier followed by a filtered DC bus is commonly adopted in order to enable bidirectional power control and improve the quality of the exchanged energy.[16]

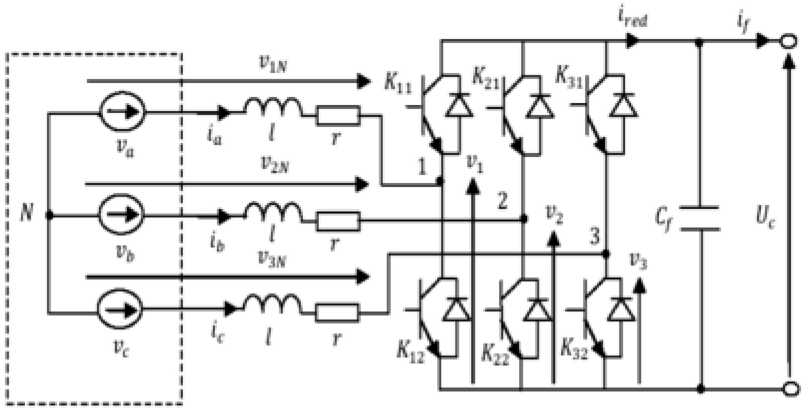

Figure II.11. Schematic Diagram of a Rectifier.

The modeling can be simplified and simulation time reduced by representing the rectifier as a set of ideal switches. These switches are complementary, and their state is determined by the following function:

$$S = \begin{cases} +1, & \overline{S} = -1 \\ -1, & \overline{S} = +1 \end{cases} \qquad \text{pour } S = a, b, c \tag{II.26}$$

Then, the input phase voltages and output current can be written as a function of:

$$i_a + i_b + i_c = 0 \tag{II.27}$$

The input voltages between phases of the PWM rectifier can be described by:

$$\begin{cases} U_{sab} = (S_a - S_b)V_{dc} \\ U_{sbc} = (S_b - S_c)V_{dc} \\ U_{sca} = (S_c - S_a)V_{dc} \end{cases} \tag{II.28}$$

II.6. Simulation of a Wind Turbine Based on a Permanent Magnet Synchronous Generator (PMSG)

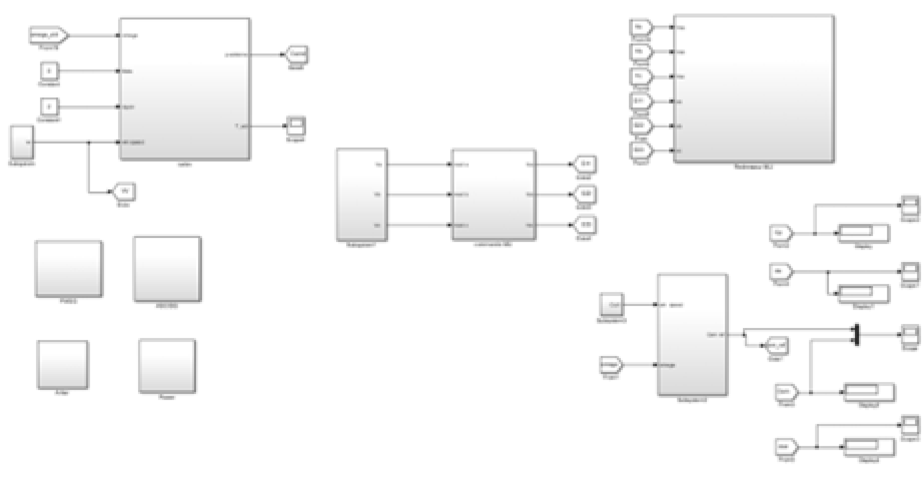

Figure II.12. MATLAB Simulation of a Wind Turbine Based on a Permanent Magnet Synchronous Generator (PMSG).

II.7. Conclusion

In this chapter, the mathematical and operational modeling of the Permanent Magnet Synchronous Generator (PMSG) was presented, along with the study of the different electrical and mechanical equations associated with it. In addition, the Park transformation and the control techniques required to analyze the system performance and improve its stability were discussed. Furthermore, the wind turbine model and the related power conversion systems, including the inverter and the rectifier, were introduced. These models constitute an essential foundation for understanding the behavior of the wind energy conversion system and for developing the control strategies that will be used later in this study.

Chapter III

Control of PMSG Using Field-Oriented Control (FOC) and PI Controllers

III.1. Introduction

This chapter constitutes a key stage in the investigation of Permanent Magnet Synchronous Machine (PMSM) control, with emphasis on vector control and on how the Proportional–Integral (PI) controller contributes to system performance. Vector control is widely regarded as a central approach in contemporary drive control because it enables decoupled regulation of torque and flux, which can improve dynamic behavior and support accurate control of speed and current.

The chapter will present the operating principle of vector control and its general architecture, together with the flux-orientation method that enables independent manipulation of current components in the dq reference frame. Particular attention is devoted to the PI controller as a primary element within the control loops; it is employed for current and speed regulation, to support closed-loop stability, and to reduce the deviation between reference commands and measured responses.

Finally, the proposed strategy is applied to a system comprising the machine and its power-electronic converter, with the aim of evaluating overall performance and examining the extent to which PI-based vector control improves operating characteristics and dynamic response.

III.2. Field-Oriented Control (FOC)

III.2.1. Presentation

Field-Oriented Control (FOC), also known as vector control, is an advanced motor control technique that enables independent control of torque and magnetic flux in AC motors. This technique is based on transforming the three-phase motor control problem into a two-phase DC-like control problem, which simplifies the control process and improves the dynamic performance of the motor. This is achieved through the use of two main mathematical transformations: the Clarke Transformation, which converts the three-phase currents (a, b, c)into two-phase stationary coordinates (α, β), and the Park Transformation, which converts these stationary coordinates into a rotating (d, q)reference frame, allowing separate and more precise control of flux and torque [25].

III.2.2. Operating Principle

The following steps outline the basic operation of field-oriented control (FOC)[24]:

1. Measure the motor current: Several approaches can be used to acquire the three-phase currents in the machine, including Hall-effect sensing, transformer-based magnetic sensors, or one, two, or three shunt resistors placed at selected locations.

2. Estimate the rotor-flux angle: The rotor-flux angle may be inferred using back-EMF-based methods or, alternatively, via high-frequency signal injection.
3. Transform the measured currents to the αβ reference frame: The measured phase currents are mapped onto two orthogonal components in the αβ frame using the Clarke transformation.
4. Transform the αβ currents to the dq reference frame: Using the estimated rotor-flux angle, the αβ components are converted to orthogonal dq components through the Park transformation.
5. Compare the measured dq currents with the reference currents and form error signals: The q-axis reference current used for torque regulation and the d-axis reference current associated with flux regulation are compared with the corresponding measured values to obtain the respective current errors.
6. Compute the control voltage from the current errors: The current-error signals are used to determine voltage corrections; in practice, this is commonly implemented as a closed-loop feedback controller based on a PI regulator.

Apply the control voltage at the motor terminals: The dq voltage commands are transformed back to the abc frame and then imposed at the motor terminals through a power-conversion stage. In many MCU-based implementations, PWM strategies, including space-vector modulation, are typically adopted for this purpose.

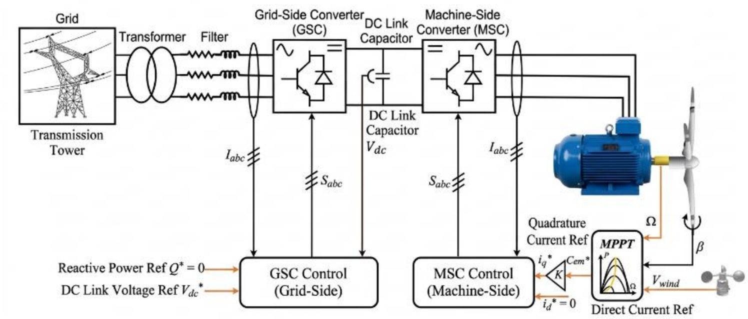

Figure III.1. General structure of the control applied to the PMSG.

III.3. The Proportional-Integral (PI) Controller

III.3.1. Definition of the PID Controller

The PID controller is a type of controller that corrects the error signal generated by the system using three distinct parameters: proportional (P), integral (I), and derivative (D) actions.

- The proportional value is proportional to the current error.
- The integral value is proportional to the integral of the error over time.

- The derivative value is proportional to the rate of change of the error.

In fact, the order of the letters or words does not necessarily reflect the sequence of the error correction process.

III.3.2. Time-Domain Equation

$$u(t) = K_p e(t) + K_i \int_0^t e\,(t)\,dt + K_d \frac{de(t)}{dt} \qquad \text{(III.29)}$$

Where:

- $u(t)$: controller output signal
- $e(t)$: error signal
- K_p: proportional gain
- K_i: integral gain
- K_d: derivative gain

III.3.3. Laplace Transform

$$U(P) = K_p E(P) + K_i \frac{E(P)}{P} + K_d P E(P) \qquad \text{(III.30)}$$

$$U(P) = E(P)\left(K_p + \frac{K_i}{P} + K_d P\right) \qquad \text{(III.31)}$$

III.3.4. Transfer Function of the PID Controller

$$C(P) = \frac{U(P)}{E(P)} = K_p + \frac{K_i}{P} + K_d P \qquad \text{(III.32)}$$

$$C(P) = K_p\left(1 + \frac{K_i}{K_p P} + \frac{K_d P}{K_p}\right) \qquad \text{(III.33)}$$

$$C(P) = K_p\left(1 + \frac{1}{T_i P} + T_d P\right) \qquad \text{(III.34)}$$

Where:

$T_i = \frac{K_p}{K_i}$ is the integral time constant (III.35)

$T_d = \frac{K_d}{K_p}$ is the derivative time constant. (III.36)

III.3.5. The Functional Block Diagram

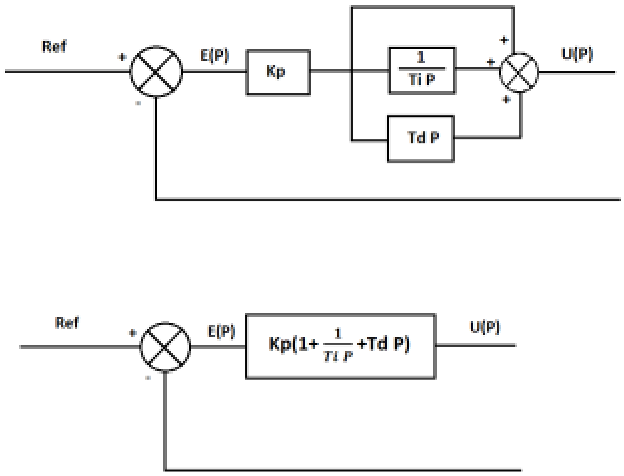

Figure III.2. Block Diagram of PID.

III.3.6. Operating Principle

The PID controller corrects errors through its three actions, where each component plays a specific role in the correction process.

- **P:** Accelerates the system response by reducing the response time through amplification of the error signal. It is adjusted using K_p.
- **I:** Improves system accuracy by eliminating steady-state errors through accumulation of the error over time. It is adjusted using K_i.
- **D:** Enhances system stability by damping oscillations and generating opposite corrective signals against rapid variations. It is adjusted using K_d.

III.4 PI Controller

The PI part is obtained from the PID controller by removing only the derivative term D, meaning we set:

$K_d = 0$

Therefore, the PI controller equation is:

$$u(t) = K_p e(t) + K_i \int_0^t e\,(t)\,dt \quad \text{(III.37)}$$

In Laplace form:

$$U(P) = K_p E(P) + K_i \frac{E(P)}{P} \tag{III.38}$$

Transfer function:

$$C(P) = \frac{U(P)}{E(P)} = K_p + \frac{K_i}{P} \tag{III.39}$$

Using the integral time constant:

$$T_i = \frac{K_p}{K_i} \tag{III.40}$$

It becomes:

$$C(P) = K_p \left(1 + \frac{1}{T_i P}\right) \tag{III.41}$$

Operationally:

P speeds up the response, and I eliminates the steady-state error.

III.5 Field-oriented control with a PI regulator for a (PMSG)

Based on the permanent magnet synchronous generator (PMSG) model in the Park reference frame presented in the previous chapter, and by using PI-type controllers within the control structure, the mathematical model equations of the permanent magnet synchronous generator can be written as follows:

$$V_{Rd} = R_s I_d + pL_d I_d - \omega\psi_q \tag{III.42}$$

$$V_{Rq} = R_s I_q + pL_q I_q - \omega\psi_d \tag{III.43}$$

The coupling terms:

$$E_{dq} = \omega\psi_{dq} \tag{III.44}$$

are considered as measurable disturbances.

The transfer function of the machine can be written in the following form:

$$G_s(p) = \frac{1}{R_s + L_s p} = \frac{1/R_s}{1 + T_e p} \tag{III.45}$$

$$G_{dq}(p) = \frac{I_{dq}(p)}{V_{dq}(p) - E_{dq}(p)} \tag{III.46}$$

With the electrical time constant:

$$T_e = \frac{L_s}{R_s} \tag{III.47}$$

The regulation loops are then represented by the diagram shown in Figure III.2 (the diagram is identical for the current loop on the q-axis).

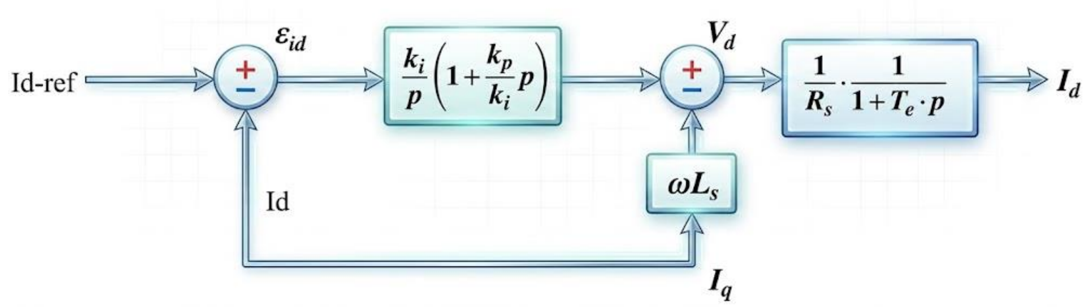

Figure III.3. Current control loop.

The open-loop transfer function is given by:

$$G_0(p) = \left(1 + \frac{k_{ci}}{p}\right)\frac{1}{k_{cp}R_s(1 + T_e p)} \tag{III.48}$$

The regulator parameters are determined using the pole compensation method.

In the open loop, the time constants are therefore equal to:

$$T_0 = \frac{k_{cp}}{k_{ci}} = T_e \tag{III.49}$$

In the closed loop, the transfer function becomes:

$$G_f(p) = \frac{G_0(p)}{1 + G_0(p)} = \frac{1}{1 + \frac{R_s}{k_{ci}}p} \tag{III.50}$$

Thus, in the closed loop, the time constant T_f is equal to:

$$T_f = \frac{R_s}{k_{ci}} \tag{III.51}$$

Therefore:

$$k_{ci} = \frac{R_s}{T_f} \tag{III.52}$$

The proportional gain k_{cp} of the regulator is:

$$k_{cp} = \frac{L_s}{T_f} \tag{III.53}$$

Figure III.3 illustrates the torque control strategy, which includes the current regulation loops and the voltage decoupling.

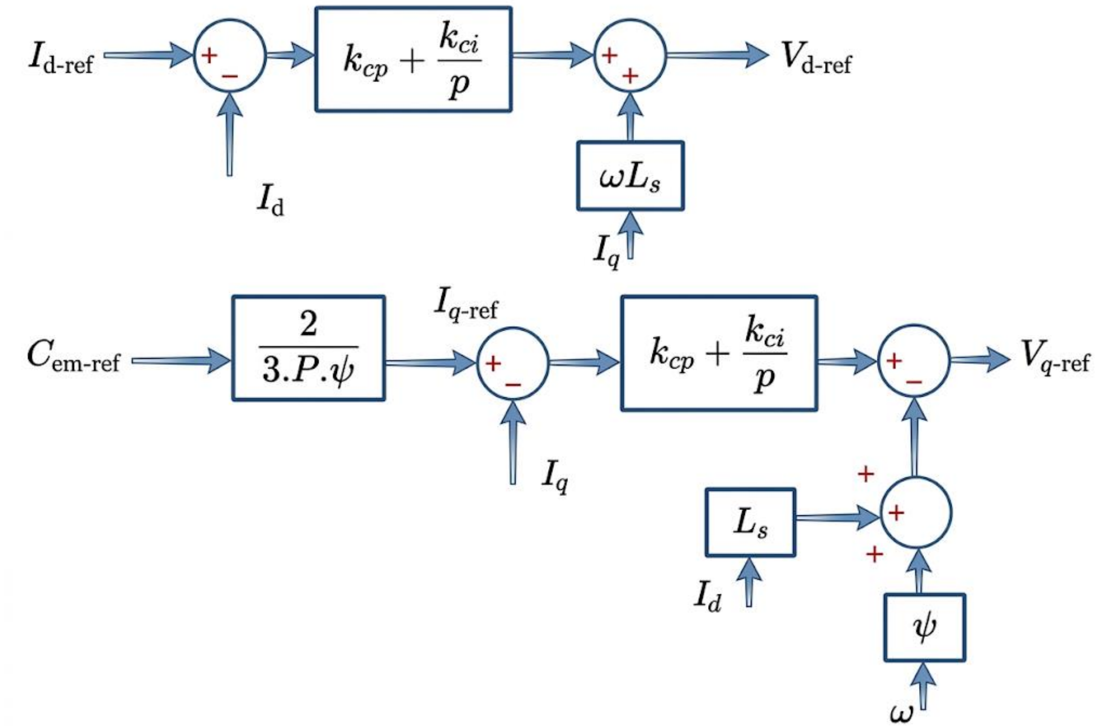

Figure III.4. Torque control strategies of the PMSG.

III.6 Complete Structure of the Vector Control of the PMSG

The reference input of the machine control is the reference electromagnetic torque C_{em-ref}

Using the previous modeling steps and the inversion rules, the following complete structure of the vector control of the PMSG is proposed Figure III.4

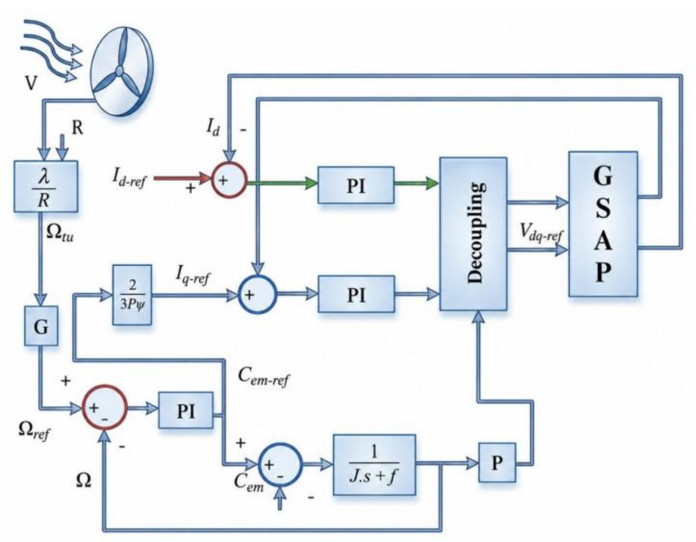

Figure III. 5. Block diagram of the vector control of the PMSG.

III.7 Simulation of the Field-oriented control of the PMSG

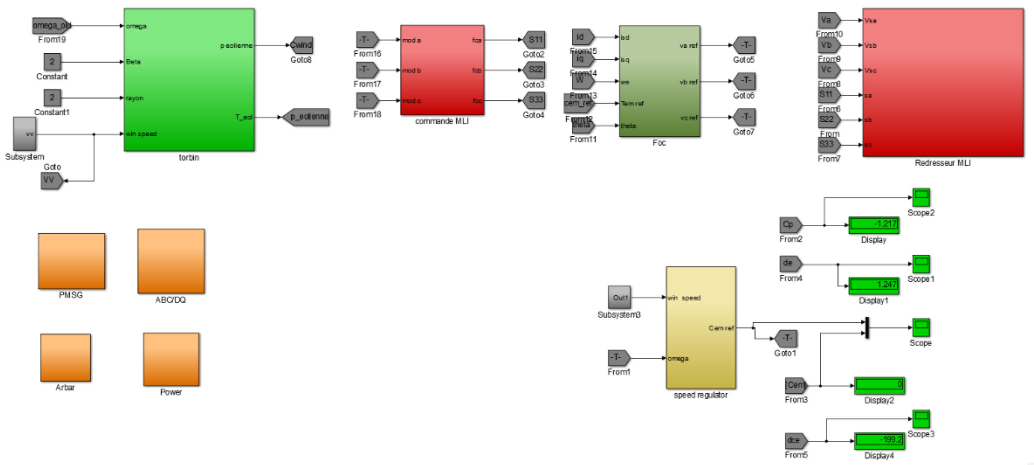

Figure III.6. MATLAB Simulation of (FOC)of the PMSG.

III.8. Simulation results

The following results illustrate the dynamic performance of the PMSG-based wind energy conversion system under variable wind speed conditions. The objective is to evaluate the effectiveness of the FOC strategy in ensuring stable operation, efficient power extraction, and proper regulation of the electrical variables.

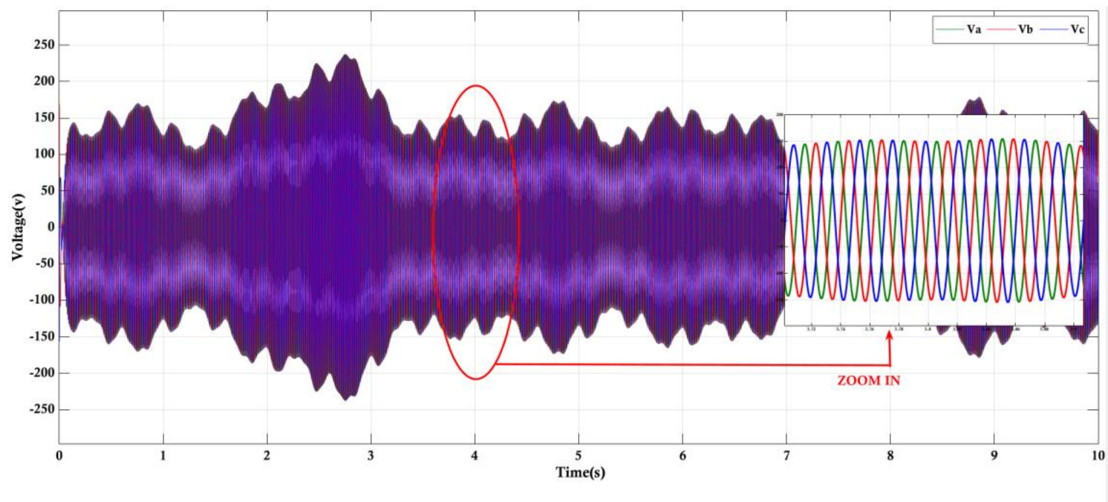

Figure III.7. simulation result of voltage (abc).

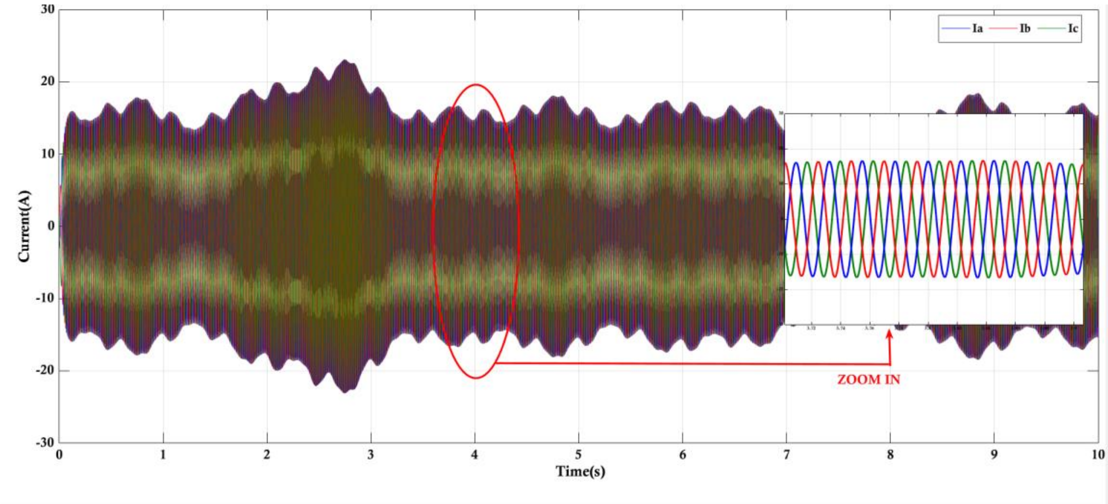

Figure III.8. simulation result of current (abc).

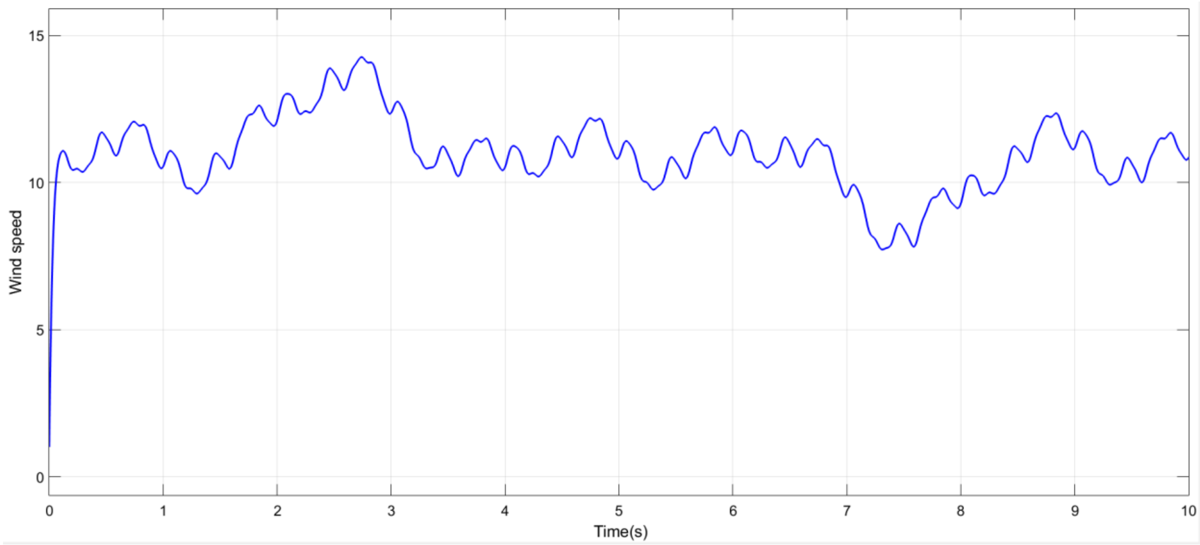

Figure III.9. simulation result of wind speed(m.s).

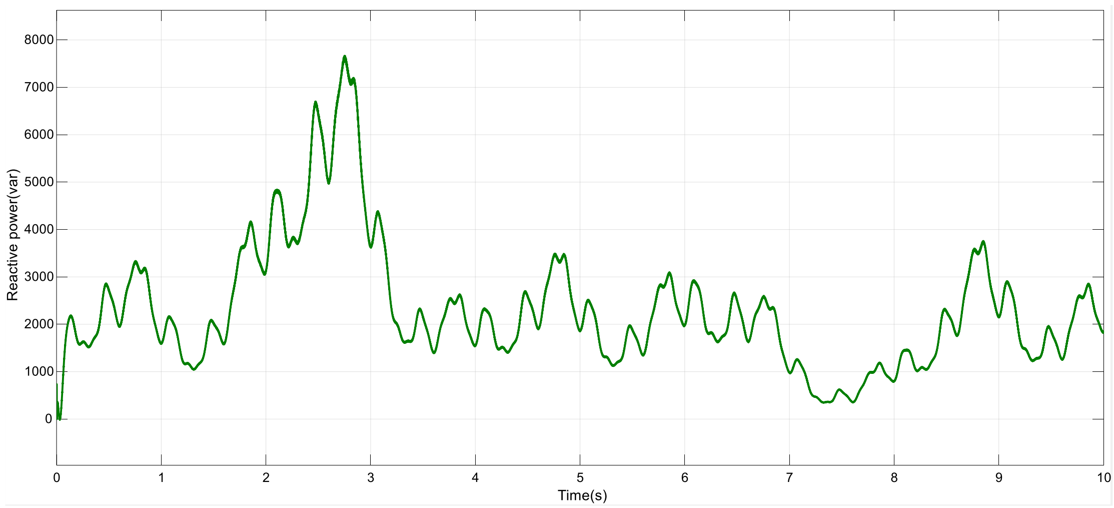

Figure III.10. simulation result of Reactive Power.

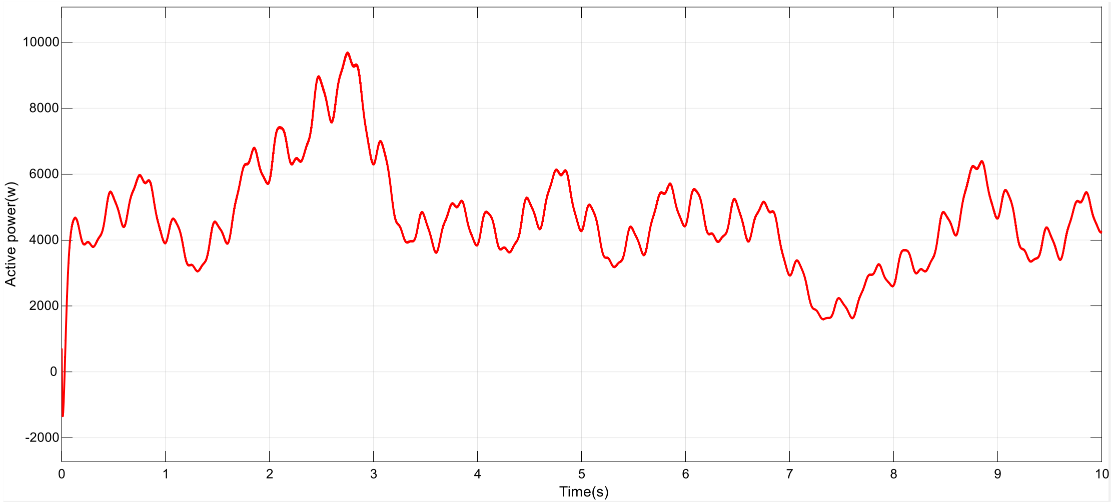

Figure III.12. simulation result of Active Power.

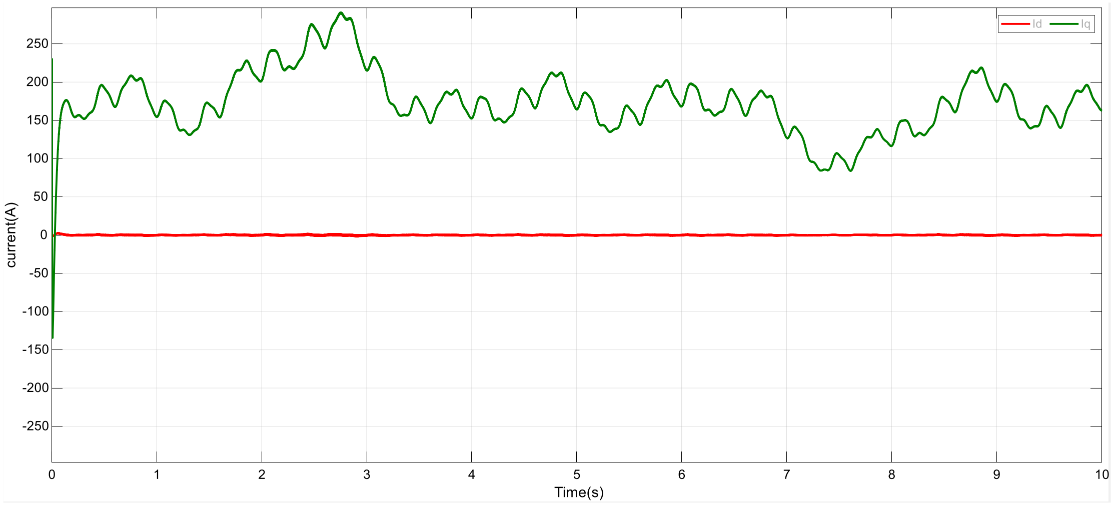

Figure III.11. simulation result of current (dq).

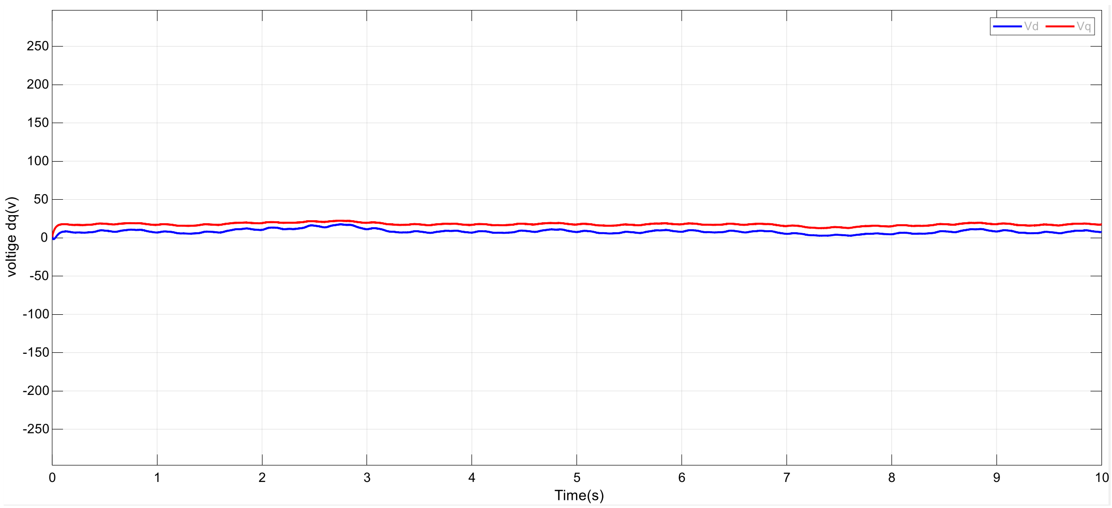

Figure III.13. simulation result of voltage (dq).

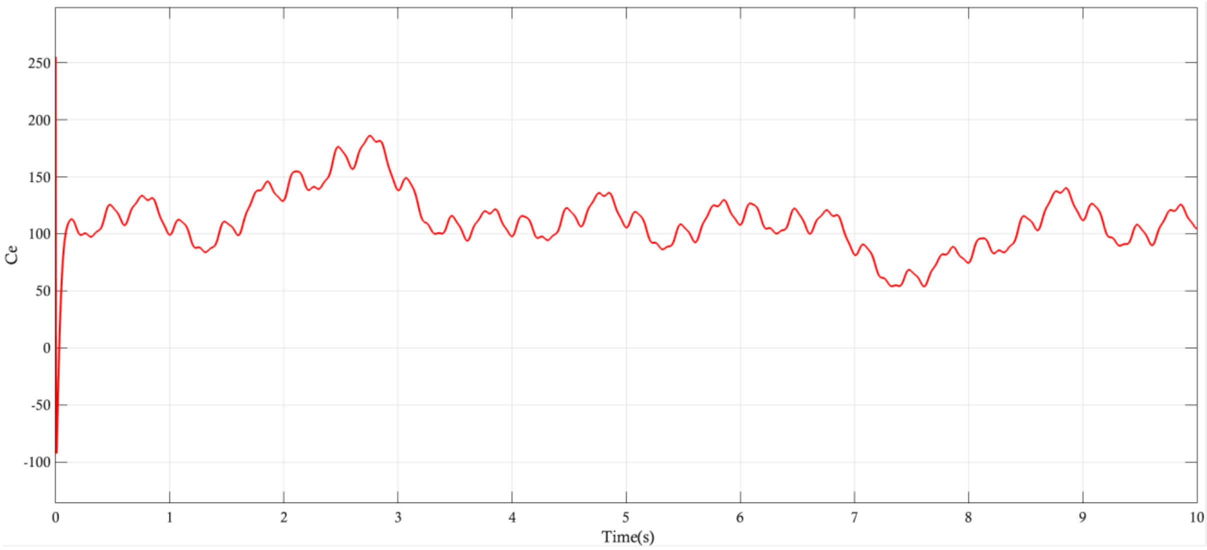

Figure III.15. simulation result of Electromagnetic Torque.

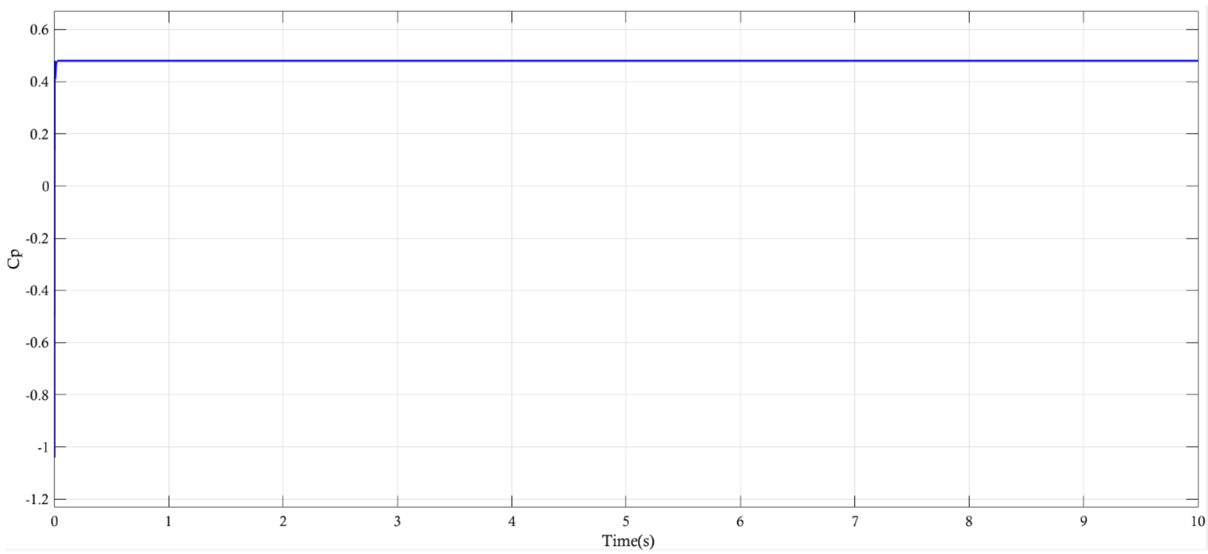

Figure III.14. simulation result of Power Coefficient (Cp).

III.9 Conclusion

This chapter presented the application of Field-Oriented Control (FOC) with PI controllers for the control of the Permanent Magnet Synchronous Generator (PMSG). The obtained simulation results demonstrated the effectiveness of the proposed control strategy in ensuring stable operation, satisfactory dynamic performance, and proper regulation of the system variables under varying operating conditions. The next chapter will focus on intelligent optimization techniques, namely Grey Wolf Optimization (GWO) and Fuzzy Logic, and their contribution to enhancing the performance and robustness of the PMSG control system.

Chapter IV

Grey Wolf Optimization and Fuzzy Logic- Based Control

IV.1 Introduction

In the previous chapter, a Field-Oriented Control (FOC) strategy was developed for the Permanent Magnet Synchronous Generator (PMSG) connected to a wind turbine in order to ensure effective regulation of the electrical and mechanical variables. Although the conventional control structure provides satisfactory performance, its effectiveness may be affected by parameter variations, system nonlinearities, and changing wind conditions. To further improve the dynamic response and robustness of the system, intelligent control and optimization techniques can be employed. Therefore, this chapter introduces Grey Wolf Optimization (GWO) and Fuzzy Logic Control (FLC) and investigates their application to the PMSG-based wind energy conversion system. The performance of the proposed approaches is evaluated through simulation under variable wind speed conditions.

IV.2 Optimization Methods

IV.2.1 presentation

Many optimization problems involve high complexity or lack analytical solutions, which has led to the development of nature-inspired optimization algorithms known as metaheuristic algorithms. These algorithms imitate the collective behavior of living organisms such as ants, birds, and wolves in order to find optimal solutions for complex problems. In general, optimization algorithms are divided into deterministic and stochastic algorithms, where stochastic algorithms are more capable of avoiding local optima due to their use of randomness and global search strategies.

Among the most popular algorithms are Genetic Algorithms (GA), Ant Colony Optimization (ACO), and Particle Swarm Optimization (PSO). In addition, the Grey Wolf Optimization (GWO) algorithm was proposed based on the hunting behavior and social hierarchy of grey wolves. This algorithm has demonstrated high efficiency and fast convergence compared to several other optimization methods, making it widely used in applications such as automatic control, power dispatch, feature selection, and multi-objective optimization problems [26].

IV.2.2 Principle of operation

Optimization is essentially everywhere, from engineering design to economics and from holiday planning to Internet routing. As money, resources and time are always limited, the optimal utilization of these available resources is crucially important.[27],[28]

In general, an optimization problem can be written as optimize $f_1(x),\ldots,f_i(x),\ldots,f_N(x)$, $x = (x_1,\ldots,x_d)$

subject to,

$$h_j(x) = 0 \ , (j = 1,2,\ldots,J)$$

$$g_k(x) <= 0 \ , ((k = 1,\ldots,K)$$

where f_1, ..., f_N are the objectives, while h_j and g_k are the equality and inequality constraints, respectively. In the case when N=1, it is called single-objective optimization. When N≥2, it becomes a multi-objective optimization problem whose solution strategy is different from those for a single objective. This article mainly concerns single-objective optimization problems.

IV.2.3 Different types of optimization algorithms

IV.2.3.1 Deterministic optimization algorithm

Deterministic approaches take advantage of the analytical properties of the problem to generate a sequence of points that converge to a globally optimal solution. These approaches can provide general tools for solving optimization problems to obtain a global or approximately global optimum.

Examples: linear programming, nonlinear programming, and mixed-integer nonlinear programming, etc.

IV.2.3.2 Heuristics and metaheuristics

A meta heuristic is a higher-level procedure or heuristic which aims to find, generate, or select a heuristic (partial search algorithm) that may provide a sufficiently good solution to an optimization problem. They are used especially when incomplete or imperfect information is available or when there is limited computation capacity.[27]

Meta heuristics make relatively few assumptions about the optimization problem being solved and so may be usable for a variety of problems.

Examples:

- Particle Swarm Optimization (PSO),
- Ant Colony Optimization (ACO),
- Genetic Algorithms (GA),
- Cuckoo search algorithm,
- Grey wolf optimization (GWO)

This article aims to introduce the basics of a novel metaheuristic called Grey wolf optimization (GWO)

IV.3 Grey wolf optimization (GWO) algorithm

IV.3.1 Identification of GWO

Grey wolf optimizer (GWO) is a population-based meta-heuristics algorithm that simulates the leadership hierarchy and hunting mechanism of grey wolves in nature, and it's proposed by Seyedali Mirjalili et al. in 2014.[28],[29]

- Grey wolves are considered apex predators, which are at the top of the food chain
- Grey wolves prefer to live in groups (packs), each group contain 5-12 individuals on average.

1. All the individuals in the group have a very strict social dominance hierarchy as demonstrated in the accompanying figure.

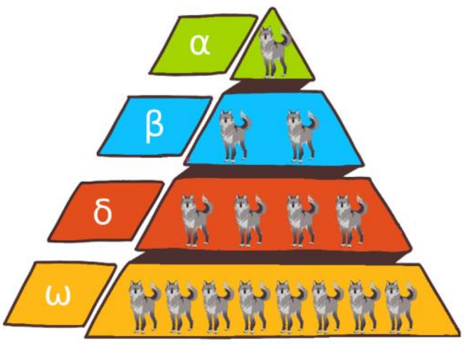

Figure IV.1. GWO hierarchical categories.

2. Alpha α wolf is considered the dominant wolf in the pack and his/her orders should be followed by the pack members.
3. Beta β are subordinate wolves, which help the alpha in decision-making and are considered as the best candidate to be the alpha.
4. Delta δ wolves have to submit to the alpha and beta, but they dominate the omega. There are different categories of delta-like Scouts, Sentinels, Elders, Hunters, Caretakers etc.
5. Omega ω wolves are considered as the scapegoat in the pack, are the least important individuals in the pack and are only allowed to eat at last.

IV.3.2 Main phases of grey wolf hunting

1. Tracking, chasing and approaching the prey.
2. Pursuing, encircling, and harassing the prey until it stops moving.

3. Attack towards the prey.

The social hierarchy and hunting behaviour of grey wolves are mathematically modeled to design GWO.

IV.3.3 Mathematical model and algorithm

IV.3.3.1 Social hierarchy

- The Fittest solution as an Alpha wolf (*α)*
- Second best solution as a Beta wolf (*β)*
- Third best solution as a Delta wolf (*δ)*
- Rest of the candidate solutions as Omega wolves (ω)

IV.3.3.2 Encircling the Prey

$$\vec{D} = | \vec{C}.\overrightarrow{X_p}(t) - \overrightarrow{X_p}(t) | \quad \text{(IV.54)}$$

$$\vec{X}(t+1) = \overrightarrow{X_p}(t) - \vec{A}.\vec{D} \quad \text{(IV.55)}$$

Where t indicates the current iteration, $\vec{A}$ and $\vec{C}$ are coefficient vectors, $\overrightarrow{X_p}$ is the position vector of the prey, and $\vec{X}$ indicates the position vector of a grey wolf. $\overrightarrow{X_1}(t+1) = \overrightarrow{X_\alpha}(t) - \overrightarrow{A_1}.\overrightarrow{D_\alpha}$

$$\vec{A} = 2\vec{a}\overrightarrow{r_1} - \vec{a} \quad \text{and} \quad \vec{C} = 2\overrightarrow{r_2} \quad \text{(IV.56)}$$

components of $\vec{a}$ are linearly decreased from 2 to 0 over the course of iterations and $\overrightarrow{r_1}$, $\overrightarrow{r_2}$ are random vectors in [0, 1].

IV.3.3.3 Hunting

In each iteration, omega wolves update their positions in accordance with the positions α, β, and δ alpha, beta, and delta because α, β, and δ have better knowledge about the potential location of prey.

$$\begin{cases} \overrightarrow{D_\alpha} = | \overrightarrow{C_1}.\overrightarrow{X_\alpha}(t) - \vec{X}(t) | \\ \overrightarrow{D_\beta} = | \overrightarrow{C_2}.\overrightarrow{X_\beta}(t) - \vec{X}(t) | \\ \overrightarrow{D_\delta} = | \overrightarrow{C_3}.\overrightarrow{X_\delta}(t) - \vec{X}(t) | \end{cases} \quad \text{(IV.57)}$$

$$\begin{cases} \overrightarrow{X_1}(t+1) = \overrightarrow{X_\alpha}(t) - \overrightarrow{A_1}.\overrightarrow{D_\alpha} \\ \overrightarrow{X_2}(t+1) = \overrightarrow{X_\beta}(t) - \overrightarrow{A_2}.\overrightarrow{D_\beta} \\ \overrightarrow{X_3}(t+1) = \overrightarrow{X_\delta}(t) - \overrightarrow{A_3}.\overrightarrow{D_\delta} \end{cases} \quad \text{(IV.58)}$$

$$\vec{X}(t+1) = (\overrightarrow{X_1} + \overrightarrow{X_2} + \overrightarrow{X_3})/3 \quad \text{(IV.59)}$$

IV.3.3.4 Attacking prey (exploitation)

When prey stops moving then grey wolf finish the hunting by attacking the prey and to mathematically model that we decrease the value of $\vec{a}$. $\vec{A}$ is a random value in the interval [-2a, 2a], where a is decreased from 2 to 0 over course of iterations.

|A|<1 force the wolves to attack the prey (exploitation)

IV.3.3.5 Searching for prey (exploration)

|A|>1 forces the grey wolves to diverge from the prey to hopefully find a fitter prey (exploitation)

Another component of GWO that favours exploration is $\vec{C}$. It contains random value between [0, 2]. C>1 emphasize the attack while C<1 deemphasize the attack.

IV.3.4 Pseudocode of the GWO algorithm

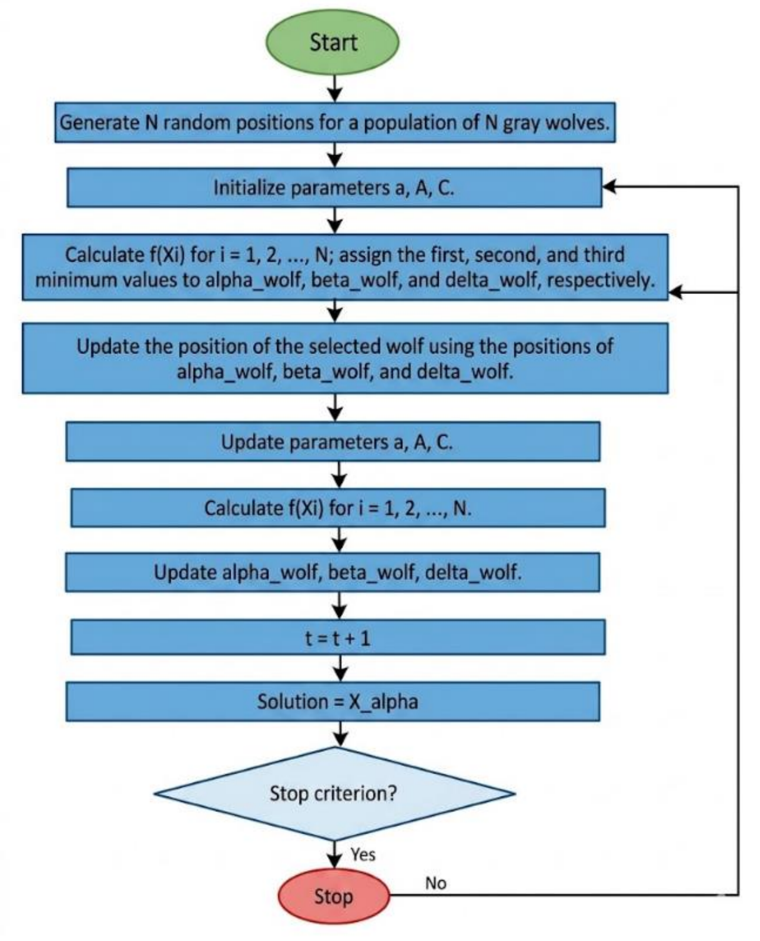

Figure IV.2. The flowchart of the GWO algorithm.

IV.5 Fuzzy logic

IV.5.1 Definition

Fuzzy logic is defined as a type of logical reasoning that involves dealing with uncertainties and vagueness rather than precision or definiteness. It is not easy in practical life to determine the accuracy of a situation's total correctness or incorrectness. Fuzzy logic is therefore useful in making decisions on such problems of uncertainty.

Boolean logic uses the number one to represent absolute correctness and zero for absolute falsity. Fuzzy logic allows partial correctness and partial falsity by allowing numbers between zero and one. The term fuzzy logic does not mean vague logic since it represents a logic system designed to handle vagueness.[30],[31]

Fuzzy logic was proposed in 1965 by Lotfi A. Zadeh in his article titled "Fuzzy Sets". This makes Zadeh the father of fuzzy logic [30]

IV.5.2 Fuzzy logic components

In general, a fuzzy logic controller (FLC) is regarded as the core element of a fuzzy control system and comprises the following four primary components: fuzzifier, knowledge base, fuzzy inference engine, and defuzzifier.

IV.5.2.1 Fuzzifier

A fuzzifier converts crisp input data (numerical data) into fuzzy values. In other words, the process starts with converting crisp input values into the fuzzy space of the controller. Following this, the inputs are categorized under fuzzy sets with proper membership functions being defined for each set.[31],[32]

IV.5.2.2 Knowledge Base:

The knowledge base is composed of two sections: the database and the rule base.

- The **database** stores the membership functions and other system parameters.
- The **rule base** contains the fuzzy rules used by the FLPSS to improve system performance.

For a system with two inputs and one output, a fuzzy rule can be expressed in the following form:

If x_1 is Fuzzy1 and x_2 is Fuzzy2, then y is $f(x_1, x_2)$.

Here, $Fuzzy_i$ represents the fuzzy linguistic terms of the inputs, while $f(x_1, x_2)$ denotes the fuzzy linguistic output.

IV.5.2.3 Fuzzy Inference

The fuzzy inference engine is regarded as the heart of a fuzzy controller since it works similarly to the way humans make judgments. Once the input information is fuzzified, the linguistic rules for the fuzzy system are employed using the inference method to derive the fuzzy output values

IV.5.2.4 Defuzzifier

The defuzzifier translates the fuzzy output into crisp numbers that can be utilized in actual situations.

Defuzzification is mathematically represented by the formula below:

$$df(x) = \frac{\sum_{i=1}^{n} x_i \, \mu_c(x_i)}{\sum_{i=1}^{n} \mu_c\,(x_i)} \tag{IV.7}$$

where:

- x_i represents the output values,
- $\mu_c(x_i)$ represents the membership function values of the fuzzy set C.

IV.6 Hybrid (GWO_ Fuzzy logic)

GWO-based fuzzy logic usually means using Grey Wolf Optimizer to automatically tune a fuzzy logic controller/system.

GWO can optimize things like:

Fuzzy logic part	What GWO tunes
Membership functions	centers, widths, triangle/trapezoid parameters
Rule base	rule weights or selected rules
Scaling factors	input/output gains
PID-fuzzy parameters	fuzzy PID gains or normalization factors

Basic workflow:

1. Define fuzzy inputs/outputs.
2. Choose membership functions and rules.
3. Encode fuzzy parameters as a GWO “wolf” solution.

4. Define a fitness function, for example error, settling time, overshoot, RMSE, or energy loss.
5. Run GWO to find the best parameters.
6. Use the optimized fuzzy controller/system.

GWO is commonly used because it has relatively few control parameters and is often applied to fuzzy controller tuning, including Takagi–Sugeno PI fuzzy controllers and power-system stabilizers.[31]

A simple formulation:

$$\min J = w_1 e(t) + w_2 OS + w_3 T_s$$

where J is the objective function, $e(t)$ is error, OS is overshoot, and T_s is settling time.

In one sentence: GWO-based fuzzy logic is a hybrid intelligent method where GWO optimizes the fuzzy system so it performs better than manually designed fuzzy logic.

IV.7 Results

IV.7.1 Simulation Conditions

In this work, the proposed wind energy conversion system was simulated using MATLAB/Simulink. The studied system is based on a wind turbine coupled to a Permanent Magnet Synchronous Generator (PMSG) controlled by Field-Oriented Control (FOC). The simulation was carried out under a variable wind speed profile during 19 s, with an average wind speed of approximately 11.75 m/s. The objective of this simulation is to evaluate the ability of the proposed control strategy to extract maximum wind power, regulate the DC-link voltage, reduce reactive power exchange with the grid, and improve the quality of the injected grid current.

IV.7.2 Comment on Simulation Results of MPPT/ limitaion based in GWO-FLC

Figure IV.3(a) shows the variation of wind speed during the simulation period. The wind speed changes continuously around an average value of about 11.75 m/s. This variable wind profile is used to test the dynamic behavior of the wind energy conversion system under changing operating conditions. The variation of wind speed allows the evaluation of the controller performance in both MPPT mode and limitation mode.

Figure IV.3(b) presents the evolution of the power coefficient Cp. It can be observed that Cp remains close to its maximum value during MPPT operation. This indicates that the wind turbine is able to extract the maximum available energy from the wind. When the wind speed increases beyond the rated value, the system moves toward limitation mode in order to avoid excessive power extraction and protect the system components.

Figure IV.3(c) shows the tip speed ratio of the wind turbine. During MPPT operation, the tip speed ratio is maintained close to its optimal value. This confirms that the control strategy succeeds in keeping the turbine operating near the maximum power point. Therefore, the turbine can achieve efficient energy conversion despite the variation of wind speed.

Figure IV.3(d) illustrates the extracted power, the nominal power, and the required power of the wind turbine system. In the MPPT region, the extracted power follows the required power reference, which confirms the effectiveness of the control strategy in maximizing the captured wind energy. When the wind speed becomes higher than the rated value, the generated power is limited around the nominal value. This limitation is necessary to protect the turbine, the generator, and the power electronic converters from overload conditions.

Figure IV.3(e) represents the reactive power exchanged with the grid. The obtained result shows that the reactive power remains close to zero during the simulation. This means that the system operates with an almost unity power factor. As a result, the proposed control strategy reduces unnecessary reactive power exchange and improves the quality of the power injected into the grid.

Figure IV.3(f) shows the DC-link voltage response. The voltage remains close to its reference value despite the variation of wind speed and the transition between operating modes. This demonstrates the ability of the control system to maintain a stable DC-link voltage. A well-regulated DC-link voltage is essential to ensure stable power transfer between the generator-side converter and the grid-side converter.

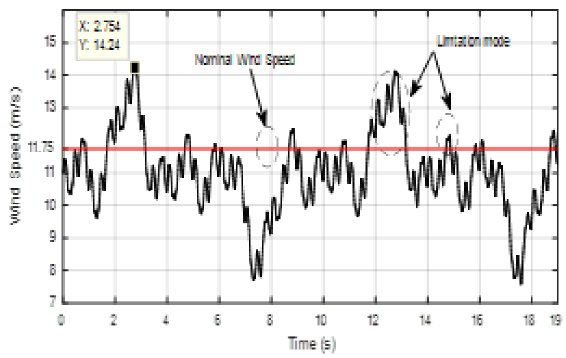

(a) Wind speed variation in (m/s)

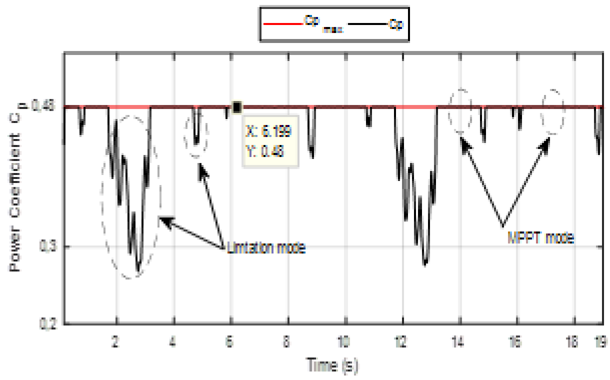

(b) the Cp

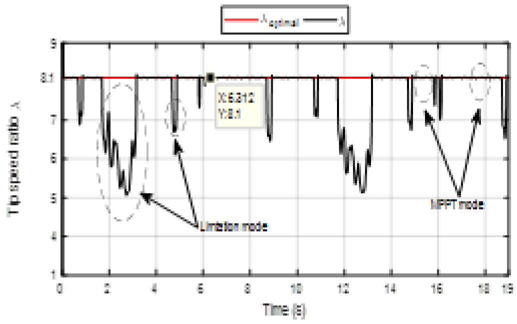

(c) the λ

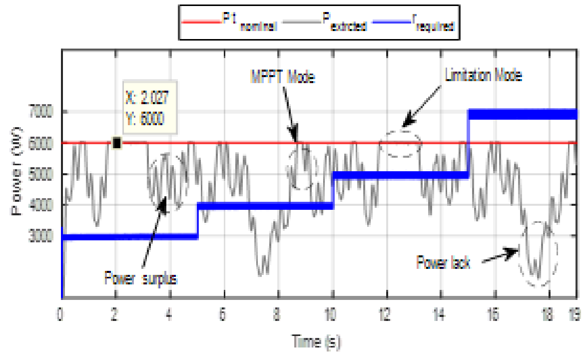

(d) The extracted, nominal and required power of the WT system

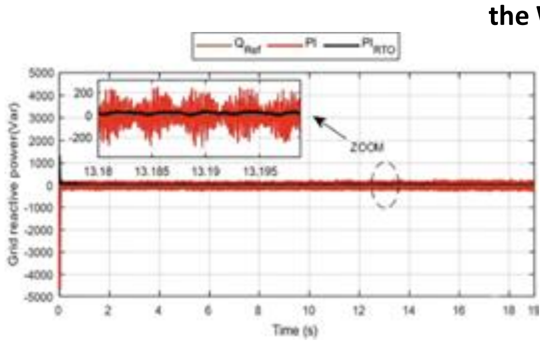

(e)Grid reactive power

Figure IV. 3. MPPT/ limitaion based in GWO-FLC.

IV.7.3 Comment on Simulation Results of DC-link Voltage

Figure IV.4 shows the DC-link voltage response for the conventional PI controller and the proposed PI-GWO-FLC controller. The reference voltage is fixed at approximately 800 V. It can be observed that both controllers are able to regulate the DC-link voltage around its reference value. However, the conventional PI controller presents larger voltage fluctuations, higher overshoot, and deeper voltage drops, especially during transient conditions.

In contrast, the PI-GWO-FLC controller shows a better dynamic response, with smaller oscillations and faster settling time. The zoomed areas clearly demonstrate that the proposed controller reduces voltage deviations and maintains the DC-link voltage closer to its reference value. This confirms the effectiveness of the PI-GWO-FLC strategy in improving voltage stability and enhancing the robustness of the system under variable wind speed conditions.

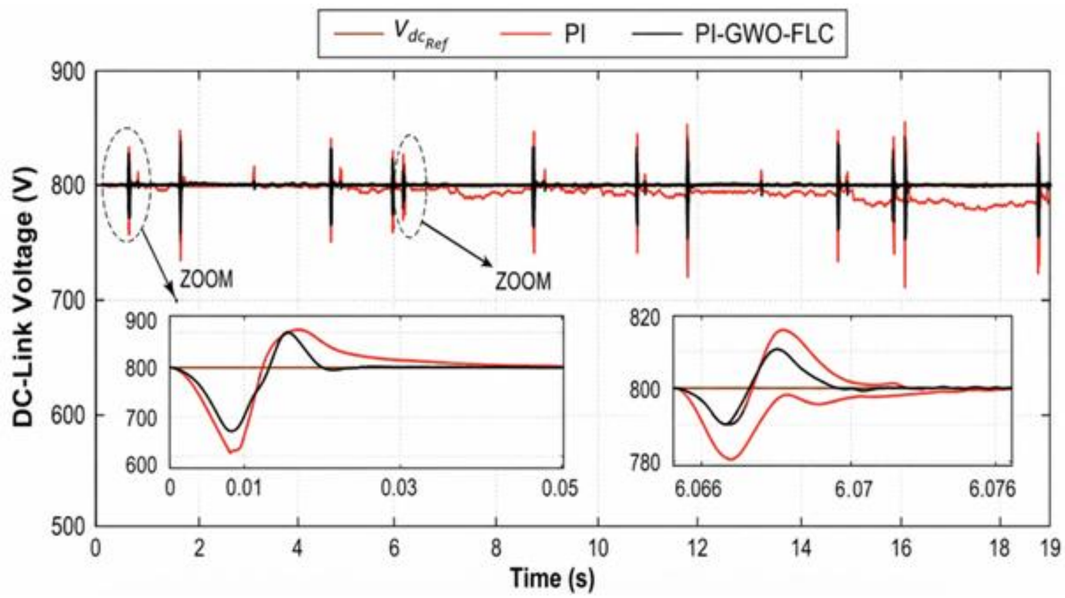

Figure IV.4. DC-link voltage.

IV.7.4 Comment on Simulation Results of Grid current for PI and (GWO-PI) and (FLC-PI) technique

Figure IV.5(a) shows the grid current obtained using the conventional PI controller. The current waveform is almost sinusoidal, which indicates acceptable current control. However, some distortions and oscillations can still be observed. This shows that the classical PI controller gives acceptable performance, but its dynamic response is limited under variable wind speed conditions.

Figure IV.5(b) presents the grid current when the PI-FLC controller is used. Compared with the conventional PI controller, the current waveform becomes smoother and closer to a pure sinusoidal shape. This improvement shows the positive effect of fuzzy logic control in enhancing the current quality and reducing distortions.

Figure IV.5(c) shows the grid current obtained using the PI-GWO controller. The waveform is more regular and closer to the ideal sinusoidal form compared with the PI and PI-FLC controllers. This result confirms that the optimization of the PI parameters using the Grey Wolf Optimization algorithm improves the dynamic response of the system and enhances the quality of the injected current.

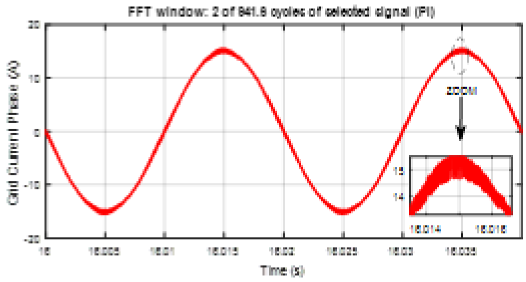

(a)Current phase"A" for PI controller

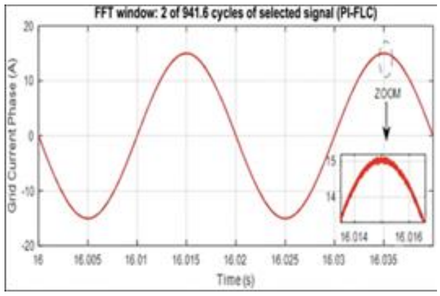

(b)Current phase"A" for FLC-PI controller

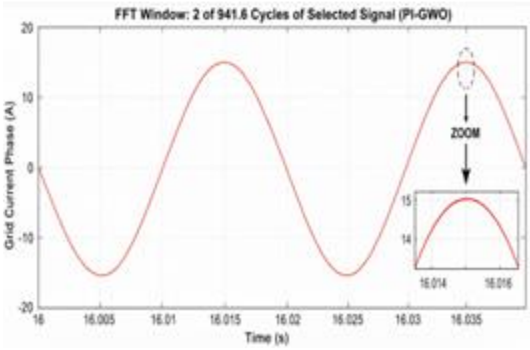

(c)Current phase"A" for GWO-PI controller

Figure IV. 5. Grid current for PI and (GWO-PI) and (FLC-PI) technique

IV.7.5 Comment on Simulation Results of Harmonic order for PI and (GWO-PI) and (FLC-PI) technique

Figure IV.6(a) presents the harmonic spectrum of the grid current using the conventional PI controller. The total harmonic distortion is about 1.79%. This value indicates that the current contains more harmonic components compared with the optimized control techniques. Although the result is acceptable, the conventional PI controller gives the highest harmonic distortion among the studied controllers.

Figure IV.6(b) shows the harmonic spectrum of the grid current using the PI-GWO controller. The total harmonic distortion is reduced to about 0.83%, which is the lowest value among the compared controllers. This confirms that the GWO-based optimization improves the tuning of the PI controller and leads to better current quality.

Figure IV.6(c) presents the harmonic spectrum of the grid current using the PI-FLC controller. The total harmonic distortion is reduced to about 0.95%. This result shows that fuzzy logic control improves the performance compared with the classical PI controller. However, its harmonic distortion remains slightly higher than that obtained with the PI-GWO controller.

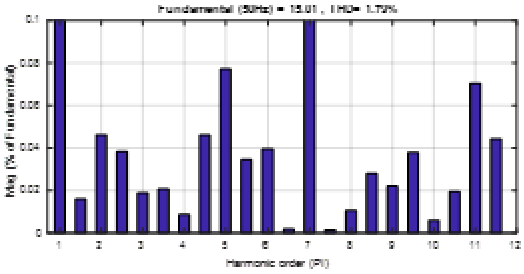

(a)Harmonic order for PI

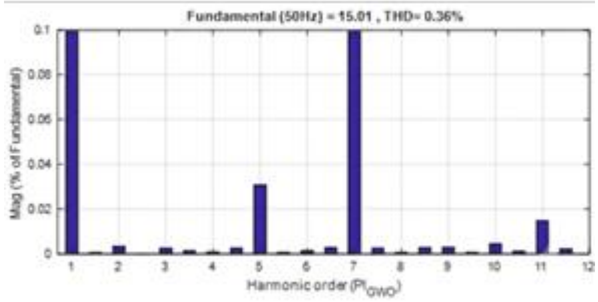

(b)Harmonic order for PI-GWO

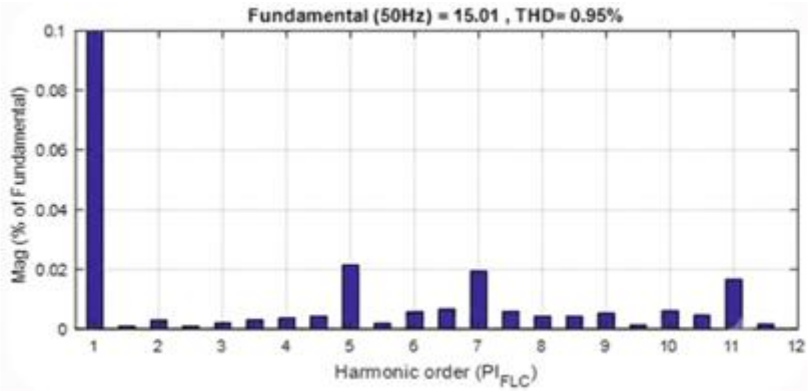

(c)Harmonic order for PI-FLC

Figure IV. 6. Harmonic order for PI and (GWO-PI) and (FLC-PI) technique

IV.7.6 Comparison Between Simulation Results

The comparison between the three control techniques shows that the conventional PI controller provides acceptable performance, but it gives higher harmonic distortion and lower dynamic quality. The PI-FLC controller improves the current waveform and reduces the THD value compared with the classical PI controller. However, the PI-GWO controller achieves the best performance, since it provides the lowest THD value and the best current waveform. Therefore, the PI-GWO controller can be considered the most effective control technique among the studied methods.

IV.8 Conclusion

This chapter presented the fundamental principles of Grey Wolf Optimization (GWO) and Fuzzy Logic Control (FLC), and their application to enhance the performance of a wind energy conversion system based on a Permanent Magnet Synchronous Generator (PMSG) controlled by the Field-Oriented Control (FOC) strategy developed in the previous chapter. The simulation results under variable wind speed conditions demonstrated that both approaches are capable of ensuring stable system operation and satisfactory control performance. Furthermore, the results showed that the GWO-based controller provides a faster response, reduced oscillations, and higher accuracy in tracking the reference values compared to the conventional fuzzy logic controller. Therefore, it can be concluded that the integration of intelligent optimization techniques with the FOC strategy significantly improves the dynamic performance and robustness of the wind energy conversion system, making GWO a promising solution for advanced control of PMSG-based wind energy systems.

General Conclusion

General Conclusion

The growing demand for electrical energy, combined with increasing environmental concerns and the progressive depletion of fossil fuel resources, has accelerated the development and integration of renewable energy systems. Among the various renewable energy technologies, wind energy has emerged as one of the most promising solutions due to its abundance, sustainability, and technological maturity. In this context, the present dissertation was devoted to the study, modeling, control, and performance enhancement of a wind energy conversion system based on a Permanent Magnet Synchronous Generator (PMSG).

The first stage of this work focused on the study of wind energy conversion systems and the modeling of the Permanent Magnet Synchronous Machine (PMSM), which constitutes the theoretical basis for the development of the generator model. The fundamental operating principles, structural characteristics, and mathematical equations governing the electrical and mechanical behavior of the machine were presented. The obtained simulation results validated the developed model and demonstrated its capability to accurately represent the dynamic performance of the machine.

Subsequently, a detailed mathematical model of the Permanent Magnet Synchronous Generator (PMSG) and the wind turbine was established. Particular attention was given to the aerodynamic conversion process, the electrical behavior of the generator, and the interaction between the mechanical and electrical subsystems. The developed model enabled a comprehensive analysis of the energy conversion process from wind energy to electrical energy and provided a suitable framework for the implementation of advanced control strategies.

To ensure efficient operation of the system, a Field-Oriented Control (FOC) strategy based on PI controllers was implemented. This control technique made it possible to achieve decoupled regulation of the electromagnetic torque and magnetic flux, thereby improving the dynamic response and control accuracy of the generator. The simulation results confirmed the effectiveness of the adopted control structure, showing satisfactory transient and steady-state performances, rapid convergence to the reference values, and stable operation under different operating conditions.

In order to further enhance the performance of the control system, intelligent control and optimization techniques were investigated through the integration of Fuzzy Logic Control (FLC) and Grey Wolf Optimization (GWO). The fuzzy logic approach provided a flexible framework capable of dealing with the nonlinearities and uncertainties inherent in wind energy systems. Furthermore, the Grey Wolf Optimization algorithm was employed to improve the tuning process and optimize the controller parameters. The comparative analysis performed under variable wind speed conditions demonstrated that both approaches ensured stable operation of the wind energy conversion system. Nevertheless, the GWO-based controller exhibited superior performance in terms of response speed, oscillation reduction, tracking accuracy, and robustness against operating condition variations.

The obtained results clearly demonstrate that the combination of a Permanent Magnet Synchronous Generator, Field-Oriented Control, and intelligent optimization techniques constitutes an effective and reliable solution for modern wind energy conversion systems. The proposed approach contributes to improving energy conversion efficiency, enhancing system stability, and ensuring better adaptation to the stochastic nature of wind resources.

In conclusion, this work confirms the significant potential of advanced control and optimization methods in improving the performance of renewable energy systems. As a perspective for future research, the proposed methodology may be extended through the implementation of hybrid intelligent control techniques, the application of other metaheuristic optimization algorithms, or experimental validation on a real-time platform in order to further assess the practical applicability of the developed solutions.

Bibliography

References

[1] Étude d'un Système Éolien à base d'une machine synchrone à aimant permanant Présenté par : LABIOD SALAH EDDINE 2022/2023

[2] Étude et réalisation d'un système éolien à base d'une machine synchrone à aimants permanents Réalisé par : M. Bouziane Medjed Eddine M. Benasmane Imad Eddine 2024

[3] Modélisation et Simulation d'une Turbine Eolienne à base d'une machine asynchrone à double alimentation (MADA) Par : Mensous Houssem Sallaye Siyyidali 2020/2021

[4] Modeling of a Wind Turbine with a Permanent Magnet Synchronous Generator for Real Time Simulations Agust´ın Tob´ıas-Gonzalez, Rafael Pe ´ na-Gallardo, Jorge Morales-Salda ˜ na, Geydy Guti ˜ errez-Urueta ´ Facultad de Ingenier´ıa Universidad Autonoma de San Luis Potos ´ ´ı San Luis Potos´ı, Mexico

[5] Ssemanda Denis, « Commande vectoriel de la machine synchrone a aimants permanents », Université SAAD DAHLAB de BLIDA, master,99pp,2015-2016.

[6] Encyclopedia of Energy 2004, Pages 191-201 Electric Motors Author links open overlay panelAnibal de Almeida [a], Steve Greenberg [b]

[7] parkingpreheater . introduction-to-permanent-magnet-synchronous-m

[8] Huang, N., "Simulation of Power Control of a Wind Turbine Permanent Magnet Synchronous Generator System", Master of Science Thesis, Department of Electrical and Computer Engineering, Marquette University, USA, 2013.

[9] Li, A., "Engineering Aerodynamic Models for Horizontal-Axis Wind Turbines", Master's Thesis, Technical University of Denmark (DTU), Denmark, 2021.

[10] Mendoza, V., "Aerodynamic Studies of Vertical Axis Wind Turbines Using the Actuator Line Model", PhD Thesis, Uppsala University, Sweden, 2018.

[11] Barakati, S. M., "Modeling and Controller Design of a Wind Energy Conversion System Including a Matrix Converter", PhD Thesis, University of Waterloo, Canada, 2008.

[12] ARIF Salim, BOUCHAALA Abdelbari, « Commande de la machine synchrone à aimant permanent (MSAP) par les réseaux de neurones artificiels », UNIVERSITE KASDI MERBAH OUARGLA,master,106pp,2018-2019

[13] https://www.wevolver.com/article/understanding-process-control-an-important-technique-for-industrial-processes

[14] YouTube channel of MATLAB. Understanding Field-Oriented Control | Motor Control, Part 4

[15] Richard M. Murray Control and Dynamical Systems California Institute of Technology

[16] Commande robuste d'une génératrice synchrone à aimant permanent (GSAP) utilisée dans une chaine éolienne . Par : HANBLI Fatima Zahra et LAIDOUNI Narimane 2024 / 2025

[17] Commande d'une génératrice synchrone à aimant permanant (GSAP) . Présenté par : MERZOUGUI Theldja /ABDELKEBIR Khedidja . 2018/2019

[18] Design of a Permanent Magnet Synchronous Generator for a Vertical Axis Wind Turbine Master of Science Thesis in Electrical Machines and Power Electronics at the School of Electrical Engineering Royal Institute of Technology Stockholm, Sweden, June 2011

[19] Commande avancé d'une Génératrice synchrone à aiment permanent intégré dans un système eolienne . Présentée et soutenue publiquement par : Laidani anouar / Litim omar abdelaziz 2023

[20] Commande vectorielle d'un générateur synchrone a aimant permanent GSAP autonome connecté aux DC micro réseaux sans système de stockage Présenté par : - CHENI Nour el islam - BAOUIAMoufid- ATOUSSi Ali 2024/2025

[21] M. MAYOUF «ETUDE comparative des architectures et stratégies de contrôle d'un aérogénérateur synchrone a aimants permanents » Université d'Al Hadj Lakhdar –Batna 2014

[22] I. Meghlaoui «Modélisation et simulation d'une chaîne de conversion éolienne de petite puissance à axe horizontal» Mémoire de magister Université Badji Mokhtar –annaba,2009.

[23] S.E. ZIRAOUI «Modélisation et étude d'un système d'énergie éolienne relié au réseau »Mémoire de master Université Badji Mokhtar –annaba 2017

[24] Sensorless Field Oriented Control for a Permanent Magnet Synchronous Motor Using Sliding Mode Observer AN4398

[25] Sensorless FOC: Techniques and Challenges by https://www.scribd.com/

[26] An Improved Grey Wolf Optimization Algorithm with Variable Weights Hindawi Computational Intelligence and Neuroscience Volume 2019, Article ID 2981282, 13 pages

[27] Mirjalili, S., Mirjalili, S. M., & Lewis, A., "Grey Wolf Optimizer", Advances in Engineering Software, Vol. 69, pp. 46-61, 2014.

[28] Li, Y., Han, M., & Guo, Q., "An Improved Gray Wolf Optimization Algorithm to Solve Engineering Optimization Problems", Sustainability, Vol. 13, No. 6, Article 3208, 2021.

[29] Benamara, K., et al., "Grey Wolf Optimization for Enhanced Performance in Wind Power Systems", Frontiers in Energy Research, Vol. 12, 2024.

[30] Abo-Khalil, A. G., Alghamdi, A. S., & Tlili, I., "Fuzzy Logic Control of Wind Energy Conversion System", Journal of Renewable and Sustainable Energy, Vol. 5, No. 2, 2013.

[31] Costa, P. J., "Fuzzy Logic as a Method to Optimize Wind Systems", In: Wind Power Systems, Springer, 2010.

[32] Maafa, A., et al., "Fuzzy Logic-Based Smart Control of Wind Energy Conversion Systems", Sustainability, Vol. 16, No. 21, 2024.

Annex

Settings of Permanent Magnet Synchronous Generator (PMSG) and Wind Turbine and GWO algorithm

$J = 0.089\ kg \cdot m^2$

$f = 0.005\ N \cdot m \cdot s/rad$

$L_d = 0.000174\ H$

$L_q = 0.000174\ H$

$R_s = 0.00829\ \Omega$

$\phi_f = 0.071\ Wb$

$P = 6$

$K = 1.5\, P\, \phi_f$

$K = 1.5 \times 6 \times 0.071 = 0.639$

$\beta = 0°$

R=2

K1=180
K2=200
K3=5000

K1=2500
K2=2500
K3=40000

K1=800
K2=800
K3=10000

$T_e = 1 \times 10^{-6}\ s$

$T_p = 1 \times 10^{-5}\ s$

$T_c = 1 \times 10^{-6}\ s$

$T_{cc} = 1 \times 10^{-6}\ s$

$T_s = 1 \times 10^{-6}\ s$

$T_{sc} = 1 \times 10^{-4}\ s$

$T_r = 1 \times 10^{-5}\ s$

$f_s = 20\ kHz$

$V_{dc} = 800\ V$

$x = 0.5$

N =30

T_{max} = 100

D = 2

f_α= Alpha score

X_α= Destination position